SESSION R

Gas Dynamics In Space Exploration

Chairman, ALFRED J. EGGERS, JR.

DR. ALFRED J. EGGERS, JR., *Chief, Vehicle-Environment Division of the NASA Ames Research Center, has contributed novel aircraft and lifting reentry concepts, and has made basic contributions to hypersonic flow theory and the understanding of spacecraft motion and heating during atmosphere entry. He has also developed specialized research equipment such as hypersonic wind tunnels and an atmosphere entry simulator. The fundamental areodynamic principle on which the RS-70 Mach 3 airplane is based was conceived by him. Dr. Eggers earned his B.A. degree at the University of Omaha in 1944, and his M.S. and Ph. D. degrees from Stanford University in 1949 and 1956, respectively. He was presented the Arthur S. Flemming Award in 1956, the Junior Chamber of Commerce Ten Outstanding Young Men Award in 1957, and the Sylvanus Albert Reed Award of the IAS in 1962. Dr Eggers is a member of the Scientific Advisory Board of the USAF, Fellow of the Institute of the Aerospace Sciences, and a member of the American Rocket Society, Sigma Xi, Tau Beta Pi, and the American Association for the Advancement of Science.*

54. Gas Dynamics Problems of Space Vehicles

By H. Julian Allen

H. JULIAN ALLEN *is Assistant Director of the NASA Ames Research Center. Mr. Allen earned a B.A. degree from Stanford University, 1932 (engineering), and a degree in aeronautical engineering from Stanford in 1935. He is a recipient of the following awards and honors: Sylvanus Albert Reed Award of the Institute of the Aerospace Sciences (1955); Distinguished Service Medal of NACA (1957): delivered Wright Brothers Lecture for the Institute of the Aerospace Sciences (1957); Airpower Trophy of the Air Force Association (1958).*

Mr. Allen is author of numerous papers on aerodynamics of atmosphere entry vehicles and ballistic missiles and on design of wind tunnels and research facilities. He is the originator of the concept of using bluntness to reduce heating of atmosphere entry vehicles; he developed supersonic theory for predicting forces and flows about bodies at angles of attack, contributed and guided the experimental investigation of heat transfer and boundary-layer development at supersonic speeds, and conceived and applied new research techniques and equipment including novel supersonic wind-tunnel nozzles, methods for visualizing airflows at supersonic speeds, and the flight-test technique of firing gun-launched models upstream through supersonic wind tunnels. He is a Fellow of the Institute of the Aerospace Sciences, a Senior Member of the American Rocket Society, and a member of Sigma Xi.

INTRODUCTION

Many space science investigations could be considered under the heading of gas dynamics. Problems concerned with the solar wind and with the interaction of planetary magnetic field with the flow of charged particles in space, while they belong in the broad sense under this province, are more appropriately treated elsewhere in this conference. Flows involved with neutral free molecules which determine the surface sputtering and the life of near-Earth satellites are certainly in the domain of gas dynamics. The present state of knowledge concerning such flows is poor despite the fact that they have long been a subject of much interest. Moreover, the so-called slip flow regime of gas flow is even less well understood. However, for lack of time, we have concentrated in this session of the conference on continuum flow problems since they are most often the gas-dynamic problems of critical importance in the space flight field. Some of the major problems have already been discussed earlier in the conference. Those discussed in this session are confined to the atmosphere entry of space vehicles with particular reference to aerodynamic heating. It is the purpose of this opening paper to discuss, first, the trajectories and speeds of entry vehicles which are of interest at present and for the future and, second, the nature of some of the problems entailed.

666582 O—62——17

26

NEAR EARTH SPACE VEHICLE PROBLEMS

When it is required to recover intact on the Earth's surface a near-Earth space probe, it can readily be shown that to effect the landing, aerodynamic braking is far more efficient from the weight standpoint than is retrorocket braking. It is well to review the fundamentals of this aerodynamic braking process. Consider for simplicity the case wherein gravity acceleration can be neglected compared to the deceleration due to drag. Then the flight trajectory is a straight line and the equation of motion is approximately

$$m\frac{dV}{dt}=-\frac{1}{2}C_D\rho V^2A \tag{1}$$

where

m vehicle mass
t time
V velocity
C_D drag coefficient
ρ air density
A characteristic area of the body

If, for simplicity, it is assumed that the enthalpy of the air is very large compared to the surface temperature of the vehicle and that the rate of radiation of heat from the vehicle to space can be neglected in comparison with the aerodynamic heating rate—assumptions appropriate for high speeds of entry—then the heat input rate is given by

$$\frac{dH}{dt}=\frac{1}{2}C_H\rho V^3A \tag{2}$$

where

H heat input
C_H heat-transfer coefficient

Combining equations (1) and (2) gives

$$dH=-\frac{C_H}{C_D}mV\,dV=-\frac{C_H}{C_D}\frac{m}{2}dV^2 \tag{3}$$

Now let us consider the case for which the ratio of heat transfer to drag coefficient is constant and assume first that the vehicle mass is constant corresponding to the case in which a heat sink is employed to absorb the aerodynamic heat generated. Then the total heat input from entry velocity, V_E, to landing is

$$H=\int_{V=V_E}^{0}dH=\frac{C_H}{C_D}\frac{mV_E^2}{2} \tag{4}$$

Now let us consider the mass to be the sum of coolant mass, m_c, the payload, m_p, and any extraneous mass, m_e, and let the heat capacity of the heat sink per unit mass expressed in kinetic energy units be ζ. Then the coolant mass is simply

$$m_c=\left[\frac{C_HV_E^2/2C_D\zeta}{1-(C_HV_E^2/2C_D\zeta)}\right](m_p+m_e) \tag{5}$$

To minimize the mass of the heat sink, then, attention must be paid to the following: The extraneous mass of the entry vehicle must be kept to a minimum (i.e., to that required for structural support in the vehicle, etc.), the heat capacity per unit mass, ζ, should be as large as possible, and the ratio of heat transfer to drag coefficient as small as possible. For velocities up to Earth circular (satellite) speed, at least, the heat-transfer process is essentially one of convection within the boundary layer. The minimum ratio of heat-transfer coefficient to drag coefficient is then generally obtained (ref. 1) by using a body shape having as high a drag coefficient as is possible, consistent with other demands.

Let us now, for comparison, consider the case wherein we replace the heat sink with an ablative heat shield which is vaporized by the aerodynamic heating experienced. One advantage long recognized for the ablative shield is that the total aerodynamic heat which can be absorbed is greatly increased by virtue of the latent heat of vaporization involved in the ablation process. A second advantage of the ablative shield (see, e.g., refs. 2 to 5) is that the issuing vapor fends off the air near the body surface within the boundary layer so as to reduce the heat-transfer coefficient itself. The reduction is approximately in the ratio (ref. 5)

$$\frac{1}{1+(KV^2/\zeta_V)} \tag{6}$$

where K depends on the molecular weight of the vapor and upon whether the boundary layer is laminar or turbulent (typically K varies in the

range 0.3 to 0.1), and ζ_V is the total energy per unit mass required to vaporize the ablator. This advantage is greater the greater the speed.

Another advantage not generally appreciated is that as the heat shield is vaporized it is automatically jettisoned; therefore, the ensuing heat load is diminished by the continuous reduction of unnecessary body mass. Thus in equation (2)

$$\frac{dH}{dt}=-\zeta_V\frac{dm}{dt}=-\frac{1}{2}C_H\rho V^3A \tag{7}$$

Combining this with the motion equation gives

$$\frac{dm}{m}=\left(\frac{C_H}{C_D\zeta_V}\right)VdV \tag{8}$$

so that if the quantity in parentheses is assumed to be essentially constant, then the mass, m, at any time when the speed is V, is related to the entry mass, m_E, and the entry speed, V_E, by

$$m=m_Ee^{\frac{C_H}{2C_D\zeta_V}(V^2-V_E^2)} \tag{9}$$

The coolant mass required is therefore

$$m_c=\left(\frac{1-e^{-\frac{C_HV_E^2}{2C_D\zeta_V}}}{e^{-\frac{C_HV_E^2}{2C_D\zeta_V}}}\right)(m_p+m_e) \tag{10}$$

which corresponds to that derived for the heat sink as equation (5).

Figure 54–1 gives the ratio of coolant mass to the payload mass (assuming the extraneous mass is zero) for an ablative heat shield obtained from equation (10) and, for comparison, the optimum corresponding ratio for a heat-sink shield (eq. (5)). For this comparison no advantage of reduced C_H and increased ζ is taken for an ablative shield in order to demonstrate the advantage of continuous mass loss due to ablation. The advantage of reducing mass by vapor jettisoning is, of course, small for our present day entry vehicles, but it will become more and more important as speed is increased. In fact, it should be noted that for the heat sink, the payload vanishes when

$$\frac{C_HV_E^2}{2C_D\zeta}=1 \tag{11}$$

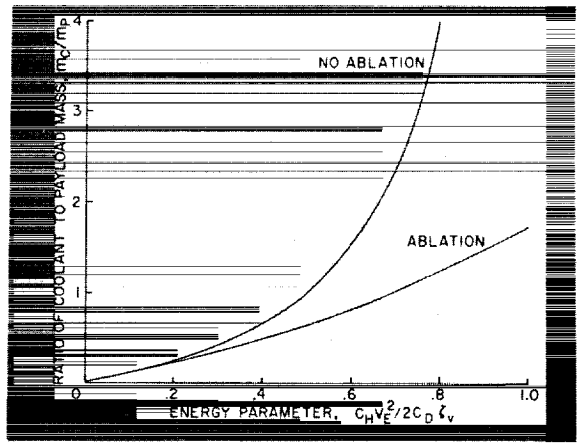

FIGURE 54–1.—Coolant mass requirements for ablative and nonablative heat shields.

but for the ablative shield the payload will not vanish regardless of the value of the ratio although for large values the fraction of total entry mass which may be payload will be uneconomically small. It is clear that the advantages for the ablating heat shield are overwhelming. In the remainder of this paper, accordingly, it is assumed that the heat shields will always be of the ablative type.

Up to this point we have considered only aerodynamic heating aspects of the entry problem. Let us turn our attention to the question of loads since, for many cases of interest, loads are a vital consideration. Again neglecting gravity the motion equation is

$$m\frac{dV}{dt}=-\frac{1}{2}C_D\rho V^2A \tag{12}$$

The trajectory is a straight line for which

$$dt=-\frac{dy}{V\sin\gamma} \tag{13}$$

where y is the altitude and γ is the angle between the flight path and the local horizontal. The air density, moreover, may be related to the altitude by the approximation

$$\rho=\rho_0e^{-\beta y}=\rho_0\bar{\rho} \tag{14}$$

where

ρ_0 sea-level density
β a constant

Thus, equation (13) becomes

$$\frac{dV}{V}=\frac{C_D\rho_0 A}{2m\sin\gamma}\,e^{-\beta y}\,dy=-\left[\frac{C_D\rho_0 A}{2\beta m\sin\gamma}\right]d\bar{\rho} \quad (15)$$

which upon integration, assuming the bracketed term is constant, yields

where
$$\left.\begin{aligned} V&=V_E e^{-\frac{1}{2}B\bar{\rho}}\\ B&=\frac{C_D\rho_0 A}{\beta m\sin\gamma}\end{aligned}\right\} \quad (16)$$

is known as the ballistic parameter.

The deceleration can be determined from equations (16) and (12) from which the unique result is obtained that if the maximum deceleration is attained before impact with the Earth (which is always the case for a vehicle that is to land intact), it is independent of the altitude at which it occurs and independent of the shape or mass of the body. The maximum value is

$$\left(\frac{dV}{dt}\right)_{\max}=-\frac{\beta V_E^2\sin\gamma}{2e} \quad (17)$$

where e is the Naperian base.

For vertical entry at Earth parabolic (escape) speed, 11.2 km/sec, the maximum deceleration is about 330 g, twice the value at Earth circular speed. Such large loads although usually permissible for instrument payloads are not acceptable for most animate payloads. As indicated by equation (17), these large decelerations can be avoided only by entering the atmosphere along a path which is nearly tangential with respect to the Earth's surface. This simple equation cannot usually be used, however, since the permissible decelerations—and this is particularly the case for manned vehicles—are not large relative to the acceleration of gravity, which is contrary to the assumption that gravity effects could be neglected. Moreover, aerodynamic lift will generally be employed to tailor the trajectory for reasons evident later. Chapman (ref. 6) has analyzed the loading problem that includes both gravity and lift in its formulation, and the numerous facets of the manned-flight problem have been treated in current literature (e.g., refs. 7 to 10).

Reduced to its essence, the problem of minimizing aerodynamic loads can be satisfactorily handled by:

(a) Stretching the total time required for entry so as to reduce the average deceleration required.

(b) Employing lift or variable drag to keep maximum decelerations near the average, or to change the trajectory after entry if the initial one would promote unacceptable decelerations.

The trajectories of interest are shown on figure 54–2 as those which are more or less tangential to the Earth surface at the beginning of entry as opposed to the near vertical entry which might be appropriate for vehicles carrying instruments only. An essential difficulty with the manned-vehicle trajectory is that the farther the vehicle goes from the Earth, the more accurate its guidance must be prior to atmosphere entry to assure that its path does not travel through levels in the atmosphere where the air is so dense that there would be intolerable decelerations. The trajectory for which the permitted maximum decleration is reached has been termed the "undershoot" trajectory. For vehicle entry at speeds greater than the Earth parabolic speed the problem is enhanced since, then, in addition, the path must pass at the other extreme through air sufficiently dense to guarantee "capture" of the vehicle by the atmosphere. That is to say, for this path the vehicle will enter and then leave the atmosphere but the exit velocity must not exceed parabolic speed or the vehicle will be lost to space. Generally the situation will have to be more restricted than has been indicated, for even if

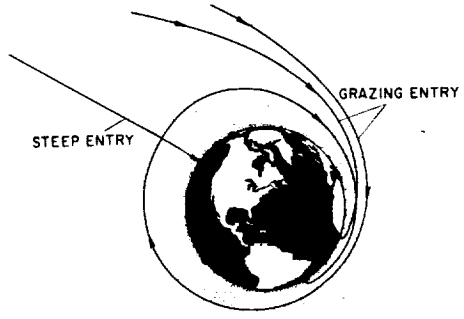

FIGURE 54–2.—Trajectories for entry into Earth's atmosphere from space.

the exit velocity is less than parabolic speed, the ensuing trajectory will entail repeated passes through the atmosphere until the speed falls below satellite speed. These digressions should not permit the manned vehicles to pass through the Van Allen radiation belts unless shielding from the lethal effects of this radiation is provided. It is usually assumed, a priori, that multiple pass entry is to be avoided. The high altitude trajectory which just meets the requirements of minimum allowed decleration has been termed the "overshoot" trajectory.

Control of lift permits alleviation of these problems in the following ways: For some entry trajectories which would entail excessive load, lift forces directed away from the Earth can be used to alter the path during entry to reduce the loads to acceptable values. On the other hand other trajectories which would provide insufficient deceleration to effect recovery in a single pass can be corrected to a single pass entry by lift forces directed toward the Earth. Figure 54–3 shows the entry corridor permitted as a function of the lift-drag ratio available for a maximum deceleration of 10 g for entry at Earth parabolic speed. The assumption here is that the lift-drag ratio is a constant for any particular trajectory. If modulation of this ratio is permitted, the incremental improvement in the corridor limits can be increased by the order of 50 percent.

Control of drag can also be used to increase the corridor height. However, lift control has the advantage that it easily permits lateral path changes near the end of the entry as landing is approached and thus assists in maneuvering to a landing point.

The introduction of lift or variable drag, in any event, complicates the problem of aerodynamic stability and requires provision for aerodynamic control. In addition, it introduces new and often objectionable facets to the problem of aerodynamic heating. The entry vehicles with relatively flat trajectories experience lower convective heat rates but for longer times. Often advantage is gained from the lower Reynolds numbers characteristic of the flatter trajectories in that laminar boundary-layer flow can be enjoyed where otherwise turbulent flow would exist. For such cases a marked reduction in heat-transfer coefficient is realized, particularly with ablative heat shields since the effect of vaporization is markedly more beneficial in reducing the heat-transfer rate in the laminar case. On the other hand, with overshoot trajectories the Reynolds number may be so low that the laminar convective heat-transfer coefficient, which varies inversely as the square root of Reynolds number, may become excessively high. In these cases although the heat-transfer rates will be decreased, the integrated heat load will be increased. This trend is shown in figure 54–4 which compares the calculated convective heating history with time for a vehicle (which for simplicity is assumed to be spherical) in vertical descent with the same vehicle in grazing trajectories at the undershoot and overshoot limits. Clearly, the integrated

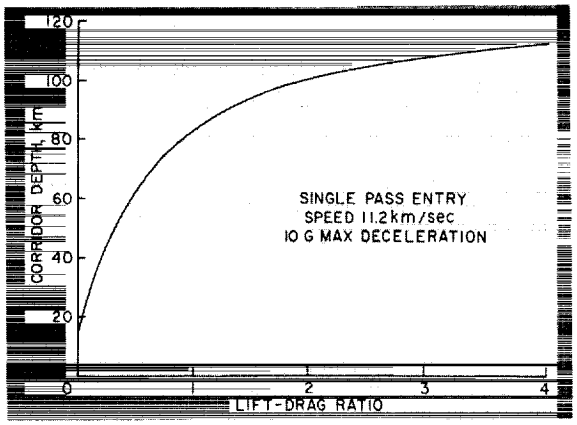

FIGURE 54–3.—Effect of lift-drag ratio on corridor depth.

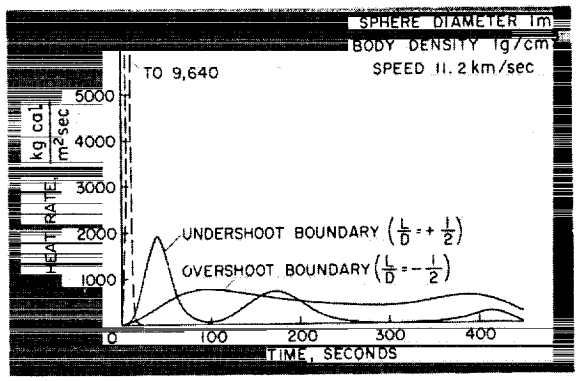

FIGURE 54–4.—Stagnation point convective heat rate for lifting spheres in grazing descent.

input for the overshoot trajectory exceeds that for the others.

All in all, the convective heating problems with the manned entry vehicles are more troublesome than those for vehicles designed for steep entry. The steep-entry vehicles always experience very high convective heating rates but for short total heating time which is a desirable state of affairs for ablative heat shields. The manned vehicles at undershoot conditions experience fairly high heat rates for reasonable short times which again makes ablative shields desirable. In overshoot conditions the lower heat rates and the longer time periods promote an increase in the absorption of heat within the ablative shield. In such cases, many otherwise suitable ablative shields will be weakened unacceptably or will soften and flow excessively. In fact, the optimum heat shields for overshoot trajectories usually are those which act in part as heat sinks and in part as radiators of heat. Thus for the manned entry vehicle, compromise in the heat-shield design is required.

Up to this point the tacit assumption has been made that convective heating constitutes the total. This is very nearly the case for entry at ballistic missile speeds, but as speed is increased, there is another source of heating which gains rapidly in importance with increase in speed. Consider a body in continuum flow at hypersonic speed. The air in the region between the shock wave and the body is drastically slowed down relative to the body in the compression process. The high kinetic energy of the stream is then almost entirely converted to heat. The translational, rotational, and vibrational modes are thus excited and, at sufficiently high speed, the energy will be enough, in fact, to dissociate and ionize a large fraction of the air in this compressed gas region. These atomic and molecular species become important sources of radiation which serve to promote additional surface heating of the entry vehicle. A chain of processes is required to establish thermodynamic and chemical equilibrium between the gas species during and following the compression transient. However, the time required for individual processes varies depending upon the reaction involved; hence, the amount of radiation emitted from elemental volumes within the gas cap is a function of the transient time. Therefore the intensity of radiation per unit volume is not constant within the gas cap but varies along streamlines. The radiative process can be visualized by reference to figure 54–5. During the initial compression immediately following A the temperature attains values approaching those corresponding to an ideal molecular gas since the translational modes of excitation of molecules are rapidly excited. As energy is diverted to the less rapid excitation of the rotational and vibrational modes and then to the relatively slow processes of molecular dissociation and to ionization, the temperature falls with time, as indicated. The early excitation of the various rotational and vibrational modes promotes the appearance and the strong upsurge of the radiation which follows the initial decline in temperature. As energy is then diverted to dissociation and ionization, the drop in temperature causes a subsidence of the radiation level until, in a short time, an equilibrium radiation level is established. By following an element of volume along a streamline, we may envision its changes of time dependent radiation intensity. If the air density in the gas cap is low, the time scale can be such that the body surface may be in the position marked B. The radiation will then be principally from the air which is not in equilibrium. On the contrary, if the gas cap density is high, the whole of the transient behavior will occur in a much shorter time and, hence, effectively farther from the body. In this case C will rep-

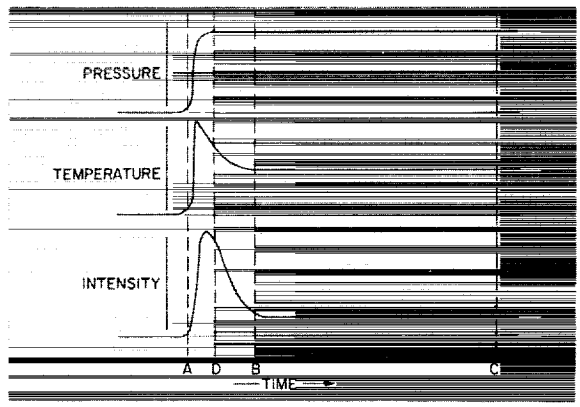

FIGURE 54–5.—Pressure, temperature, and radiation intensity history during shock compression.

resent the position of the body so that the radiation received may be well approximated by the equilibrium value as the integrated mean, provided the density is not so high that strong reabsorption of the radiation occurs within the gas layers. Reabsorption reduces the radiative heating from the value it would otherwise have.

In order to predict radiation effects and to understand experimental radiation data it is obvious that the aerodynamicist must now have much more than a passing acquaintance with the various disciplines of high-temperature physics. The gas dynamics of radiative systems has for some time been a field of interest to the astrophysicist concerned with the internal construction of stars and the radiation from them. The pioneering work of Homer Lane, Emden, and Eddington established a field of investigation that has now reached an advanced state of development (see, e.g., refs. 11, 12, and 13).

An intensive effort, both theoretical and experimental, has been made in recent years to understand the phenomenon of air radiation as it applies to atmosphere entry of space vehicles (see, e.g., refs. 14 to 18). The phenomenon is complex and far from completely understood from theoretical aspects. Moreover, the experimental investigations have not been carried far enough within the regimes of speed, air density, and body size to permit rigorous formulation of scaling laws or accurate appraisals of the levels of the equilibrium and nonequilibrium components of radiation in all cases of interest. What is known quantitatively of the entry radiative heating problem is the subject of a paper to follow, so the remarks here will be restricted to a discussion of the general aspects of the radiative heating problem and the relation of the radiative to the convective contributions for bluff bodies.

With reference to the nonequilibrium radiation, the chemical and excitation processes that occur are nearly all binary reactions (ref. 14). The time required for such reactions is inversely proportional to frequency of collisions. Therefore the thickness of the nonequilibrium layer varies inversely with density. On the other hand, the local magnitude at corresponding locations varies directly as the density. Thus for an arbitrary entry body the total nonequilibrium radiation is independent of density, although it is a function of velocity and is proportional to the cross-sectional area of the body and to its shape. The nonequilibrium contribution to the heat-transfer coefficient for a body of given shape is therefore

$$C_{H_n}=\frac{dH/dt}{\frac{1}{2}\rho V^3 A}\sim\frac{\varphi(V)A}{\frac{1}{2}\rho V^3 A}\sim\frac{\Phi(V)}{\rho} \qquad (18)$$

where φ and Φ are functions of flight speed.

With reference to the equilibrium radiation, this contribution is not only a function of velocity but also of density. For parabolic entry speed or less and for near normal bow shock compression the experimental data indicate this contribution varies approximately as the density to the 1.7 power. In addition, the total radiation emitted by the gas cap of an entry body is proportional to the volume of the gas cap which, in turn, is proportional to the body volume (i.e., $A^{3/2}$) at any given speed. Thus the equilibrium radiation contribution to the heat transfer is

$$C_{H_e}=\frac{dH_E/dt}{\frac{1}{2}\rho V^3 A}\sim\frac{\psi(V)\rho^{1.7}A^{1.5}}{\frac{1}{2}\rho V^3 A}\sim\Psi(V)\rho^{0.7}A^{0.5} \qquad (19)$$

where $\psi(V)$ and $\Psi(V)$ are functions of flight speed.

The convective heat-transfer contribution is dependent upon whether the flow is laminar or turbulent in the boundary layer and whether vapor ablation occurs, but, at hypersonic speeds, the magnitudes are in question (refs. 19, 20, and 15). For laminar flow, as is well known (e.g., see ref. 21) the heat-transfer coefficient is inversely proportional to the square root of Reynolds number; while in turbulent flow, the Reynolds number dependence is much reduced. The attenuation of the heat transfer due to vapor blowing within the boundary layer is a function of velocity but not density. Thus the convective heat-transfer coefficient is

$$C_{H_c}\sim F(V)\rho^{-\frac{n}{2}}A^{-\frac{n}{4}} \qquad (20)$$

where $F(V)$ is a function of flight speed and the exponent n is unity for laminar flow but much smaller than unity for turbulent flow.

Now it was noted earlier that the level of heat input is determined by the ratio of heat-

transfer coefficient, C_H, to the drag coefficient, C_D. For bluff bodies the drag coefficient at hypersonic speeds in continuum flow is essentially independent of speed and density. Thus summing the components

$$\frac{C_H}{C_D}\sim\Phi(V)\rho^{-1}+\Psi(V)\rho^{0.7}A^{0.5}+F(V)\rho^{-0.5n}A^{-0.25n} \tag{21}$$

From this proportionality it is clear that C_H/C_D attains a minimum for some value of air density, for if the density is increased from this value, the equilibrium radiation increases C_H/C_D more than the sum of the convection and nonequilibrium radiation decreases it, and conversely.

To illustrate this compensating influence of density, figure 54–6 shows the estimated values of the total ratio of heat-transfer coefficient to drag coefficient and the individual contributions from the several heating sources as a function of altitude for an ablating sphere of 1 meter radius moving at a speed of 10 km/sec.[1]

These curves are shown as solid lines where the estimate is reasonably reliable. The dotted portions indicate that the estimate is unreliably high for the following reasons:

(a) Convective Heating.

Between the slip flow regime and the free molecule regime an estimate which assumes laminar continuum flow (eq. (20)) yields values which increase indefinitely as density is decreased. Clearly, the ratio cannot exceed a value of about one-half since, by Reynolds analogy, if all the drag of the body were due to frictional forces, only one-half of the heat generated could enter the body. The other half must be retained by the air in the wake. In fact, in free-molecule flow a similar limitation exists. Suppose the collision of the moving body surface with the stationary air molecules were to release all of the collision energy to the body. The mass of air involved in the collisions is in unit time

$$\rho VA \tag{22}$$

The total rate of release of energy, then, is

$$(\rho VA)\frac{V^2}{2}=\frac{\rho AV^3}{2} \tag{23}$$

so that C_H cannot exceed unity. On the other hand, the drag force experienced by the body in this case is simply the momentum exchange

$$(\rho VA)V=\rho V^2A \tag{24}$$

That is, for such an energy release the drag coefficient must be 2; hence, the same limit for C_H/C_D of one-half is obtained.

(b) Radiative Heating.

Here, again, an upper bound for C_H/C_D is indicated, for suppose all of the energy

$$DV=\left(\frac{C_D}{2}\rho V^2A\right)V=\frac{C_D}{2}\rho V^3A \tag{25}$$

were to appear as radiant energy in the gas cap. If the one-half is radiated forward to space then only the other half of this energy is accepted by the body; hence,

$$\frac{1}{2}\left(\frac{C_D\rho V^3A}{2}\right)=\frac{C_H}{2}\rho V^3A \tag{26}$$

or

$$\frac{C_H}{C_D}=\frac{1}{2} \tag{27}$$

There are, in addition, other limiting factors which serve to reduce the individual radiative contributions.

[1] The convective heat transfer is that for a nonablating surface so that these results are applicable only for a heat-sink type of heat shield.

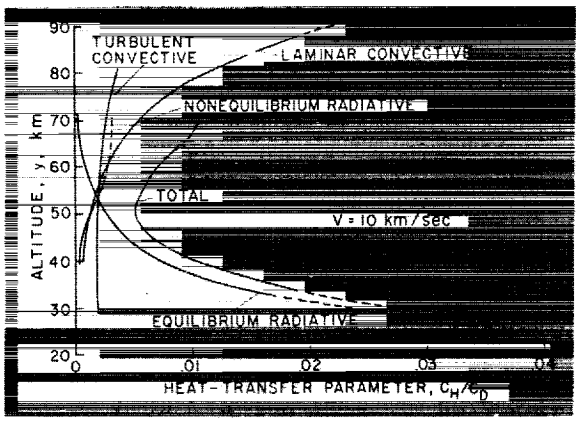

FIGURE 54–6.—Estimates of total and component heat-transfer coefficients for a sphere at 10 km/sec.

(1) Nonequilibrium radiation

In equation (18) all the nonequilibrium radiation is assumed to be released to the body when, in fact, if the collision proceeds at such a slow rate that the air passes through the compression region and expands to low density and temperature before the nonequilibrium radiant energy release is complete, the radiation will be prematurely quenched and the radiant energy release is less than estimated. This situation is equivalent to the case where the body position in figure 54–5 is D. This limiting phenomenon is thus a truncation process.

Another factor which serves to limit the nonequilibrium radiation is termed "collision limiting" (ref. 15). This occurs when the air density in the gas cap is so low that there are not enough collisions to maintain the population of particles in excited states against the drainage by radiation. Present estimates are that effects of collision limiting occur as altitude exceeds about 50 km.

(2) Equilibrium radiation

In equation (19) for equilibrium radiation each layer of the gas within the gas cap is tacitly assumed to be nearly transparent to the radiation from neighboring layers. As air density is increased, the gas becomes less and less transparent to its own radiation. Thus when strong absorption exists, the radiative heat, as noted earlier, must diminish from what it would be for an essentially transparent gas under the same conditions, and if the air density becomes sufficiently high, the gas cap radiates essentially as a black body at the equilibrium temperature corresponding to the density within the gas cap.

Let us now return to a discussion of the relative importance of the radiative and convective contribution to aerodynamic heating during entry in the speed range of near-Earth space vehicles (7 km/sec$<V<$11 km/sec). For a manned vehicle the sphere of 1 meter radius might be considered representative and for entry at Earth parabolic speed the maximum radiative heating would occur approximately at the speed of 10 km/sec when the altitude of the flight trajectory would be of the order of 60 km. At this speed and in this altitude range (fig. 54–6), the combined radiative heating is somewhat higher than the convective contribution. For the whole of the flight trajectory, however, the convective contribution would well outweigh the radiative since the convective heat-transfer coefficient is not greatly affected by change in speed. The levels of the radiative contributions are very sensitive to speed and so drop rapidly in the later stages of the entry trajectory.

For grazing trajectories, had we assumed a somewhat lower entry speed, the total radiative contribution, because of its extreme sensitivity to speed, would have been markedly reduced. On the contrary, an increase of entry speed above parabolic speed by a few kilometers per second will reverse this state of affairs.

For entry vehicles in steep descent, the speed is relatively greater at lower altitudes than it would be for a grazing trajectory. The equilibrium radiative heat transfer therefore tends to dominate the convective transfer even at parabolic speeds.

It was noted earlier that when convective processes only are important in aerodynamic heating, the heating problem for an ablative heat shield is related to the materials involved. When, in addition, radiative processes become important the relationship becomes so intimate that one cannot treat the one without full consideration of the other. It is worthwhile to note here two of the more important considerations that must be given to the cross coupling which occurs: First, certain ablative materials that have excellent qualities when convective transfer is the sole source of heating are not attractive, per se, when radiative heating is superimposed. Quartz, for example, is transparent to a wide range of radiative wavelengths and, in the presence of strong radiation, transmits this radiation to the structure supporting it, which, clearly, is most undesirable. Another material, having a similar characteristic, though it is not obvious at first thought, is a polytetrafluoroethylene known as "Teflon." This material is opaque to visual radiation at temperatures up to 600° K. A phase change occurs then and the material becomes transparent. Of course, the transparency fault can generally be corrected by introducing additives during manufacture which will promote opacity. Another

solution which suggests itself would be to introduce, as an additive, small flakes of highly reflective metals so oriented as to reflect the radiation back out of the shield. If the transmissivity of the base material and the reflectivity of the additive were both high, such a composite might serve to reduce the heating component resulting from gas radiation. This solution has, to my knowledge, never been attempted. In keeping with this approach, Howe (ref. 22) has suggested the use of ablative materials which are opaque in the vapor state. He noted that the vapors of common materials will not provide such characteristics except to a trivial degree. His idea is a novel one, however, and deserves further consideration. Second, some ablative materials contain chemical constituents which, in the vapor state, can become sufficiently excited that they add to the radiative heat input when the flow enthalpy and total heating rate are high. Carbonaceous materials are offenders in this regard.

From the foregoing discussion of aerodynamic heating and of the reaction of materials to it, we can conclude on the basis of our present knowledge that advance to Earth hyperbolic speed brings us to a new regime, a regime in which considerations of radiative heating will dictate the philosophy of design for entry vehicles. The change in point of view will have a more far reaching influence on the course of hypersonic aerodynamics, I believe, than is immediately apparent.

THE DEEP SPACE VEHICLE—PROBLEMS OF THE FUTURE

Space vehicles of the future which will become of increasing interest are those intended for journeys to distant points in the solar system. It will be desired to return to Earth some which are unmanned as well as those which are manned. Since it is anticipated that aerodynamic drag will be employed to brake the approach to Earth, the likely speed of the approach prior to entry to the atmosphere is of first concern to the aerodynamicist in that it fixes the scope of interest.

For vehicles intended for journeys to our neighboring planets, Mars and Venus, it is well known that if one employs a near-minimum

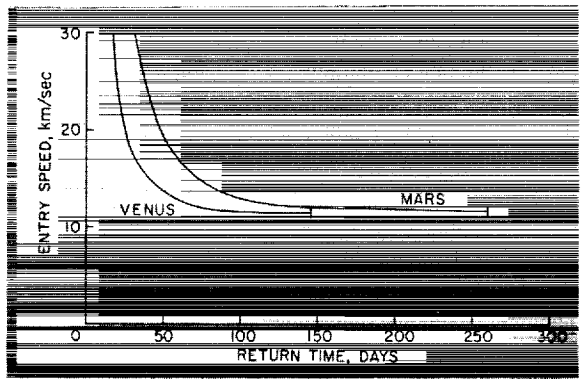

FIGURE 54–7.—Earth entry speed for minimum transit time from Mars and Venus.

energy trajectory—that is, by essentially following the Hohmann transfer ellipses—the speed of return to Earth need not be much in excess of Earth parabolic speed. The question therefore arises, "What is to be gained by employing higher speed vehicles?" The answer is simply that near-minimum energy trajectories are too time consuming as indicated in figure 54–7. A reasonably short transit time will not only be usually desired for its own sake but can effect reductions in total vehicle mass at takeoff in many cases. Shorter transit time, for example, decreases the masses involved in life support systems, in radiation shielding when accumulative exposure is a pertinent factor, and in structure required to resist, with some specified probability, the damage resulting from meteoroid impact. With reference to Earth return of such unmanned vehicles as those intended for scientific probing of the vicinity of the Sun, the aerodynamicist must contend with the entry speeds shown in figure 54–8. In short, for future vehicles we may find entry speeds far in excess of Earth parabolic speed to be of interest.

Let us turn now to the subject of aerodynamic loads imposed on vehicles in Earth atmosphere entry. For instrument payloads, as discussed earlier, steep entry trajectories are usually desired. At the higher speeds characteristic of the deep space vehicles, however, the loads may well be limiting considerations. This is apparent from the magnitude of the decelerations shown in figure 54–9.

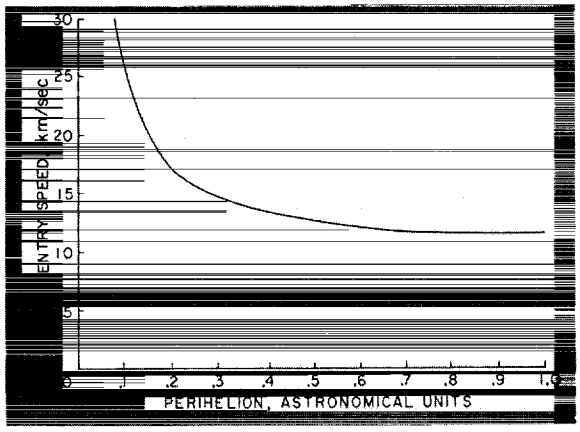

FIGURE 54–8.—Earth entry speed for a solar probe.

For manned vehicles the restrictions are considerable. If one assumes that decelerations must be limited to ten times the Earth gravity acceleration, then even if with the maximum benefit of lift (i.e., $L/D \to \infty$), the entry corridor height attainable, as shown in figure 54–10, would vanish at an entry speed of 26 km/sec. This limiting entry speed is determined in the following way: The lift force directed toward the Earth must equal the centrifugal force less the gravitational pull or

$$L=\frac{mV^2}{R}-mg \tag{28}$$

where R is the Earth radius. Hence if G is the multiple of Earth gravitational acceleration permitted

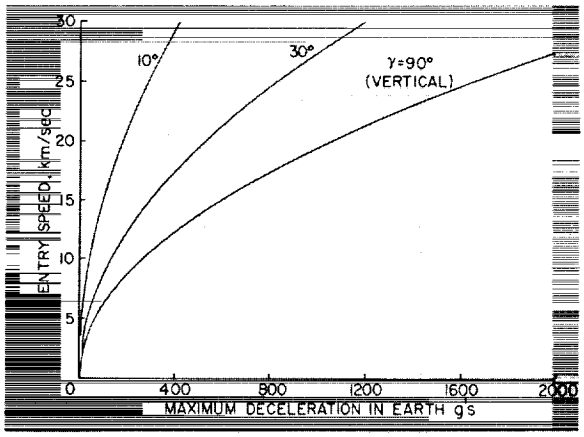

FIGURE 54–9.—Maximum decelerations as a function of Earth entry speed and entry angle.

$$G=\frac{V_{\text{lim}}^2}{gR}-1=\frac{V_{\text{lim}}^2}{V_s^2}-1 \tag{29}$$

where V_{lim} is the limiting speed and V_s is the Earth satellite speed. The limiting speed is therefore

$$V_{\text{lim}}=V_s\sqrt{G+1}=7.9\sqrt{G+1}\,\text{km/sec} \tag{30}$$

Of course, this limiting speed is an unrealistic upper bound since no drag is assumed to occur and thus the entry time is indefinitely long. These results establish the fact that for manned vehicles when transit times for space journeys become very short, it will be necessary to resort to rocket braking, at least in part, to effect an Earth landing.

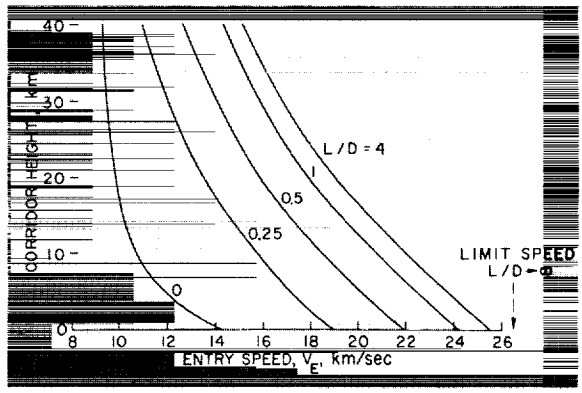

FIGURE 54–10.—Entry corridor height as a function of entry speed and vehicle lift-drag ratio.

Many interplanetary journeys will, of course, entail landings on planets other than Earth, so that gas dynamic problems associated with high-speed entry into such atmospheres form a new field of interest in hypersonic gas dynamics. Chapman (ref. 6) has given consideration to the problem of such entries. Generally, the aerodynamic loads follow the same functional relations with velocity and atmospheric density as for entry into the Earth's atmosphere but the change in atmospheric properties and, in some cases, the change in planet size and mass must be taken into account. Pertinent approximate characteristics for some near-Earth planets and for Titan, a satellite of the planet Saturn which has an atmosphere, are given in table 54–I.

TABLE 54–I.—*Approximate Characteristics of Some Planetary Bodies and Titan*

Planet	Orbit radius from Sun, km	Planet radius, km	Atmosphere density scale factor β^{-1}, km	Surface gravity acceleration, m/sec²	Surface satellite speed, km/sec	Surface parabolic speed, km/sec	Atmosphere density at surface, kg/m³	Principal atmospheric gases
Venus	1.082×10^8	0.619×10^4	6. 1	8. 53	7. 27	10. 26	2 ± 1	CO_2, N_2
Earth	1.495×10^8	0.637×10^4	7. 16	9. 806	7. 90	11. 17	1. 225	N_2, O_2
Mars	2.278×10^8	0.340×10^4	18	3. 73	3. 56	5. 03	. 1	N_2, CO_2
Jupiter	7.876×10^8	6.96×10^4(?)	18	25. 8(?)	42. 4(?)	59. 9(?)	--------	H_2, CH_4
Titan	14.25×10^8	0.210×10	30	2. 16	2. 13	3. 01	--------	CH

TABLE 54–II.—*Approach Speed and Deceleration*

Planet	Speed for Hohmann transfer from Earth, km/sec	10 g limit speed, km/sec	Deceleration for vertical entry with Hohmann transfer, Earth g
Venus	10. 5	25. 7	340
Earth	(11.2) parabolic speed	26. 2	(329) for parabolic entry speed
Mars	5. 8	18. 6	35
Jupiter	60. 2	92. 9	3780
Titan	6. 4	14. 5	26

Generally, atmosphere entry decelerations for grazing trajectories and entry corridor heights for Venus and Jupiter are about the same as for Earth. For Titan and Mars, entry is far easier to effect from the loads standpoint. For grazing trajectories, the limit speed for magnitude of deceleration equal to 10 Earth gravity accelerations as well as the minimum speed of approach corresponding to Hohmann transfer is given in table 54–II.

The last column of table 54–II gives the deceleration in Earth g units for vertical atmosphere entry. Again Mars and Titan represent a one order magnitude reduction in loading compared to Venus and Earth (listed for Earth parabolic speed) vertical entry. Note that for vertical descent, Jupiter entry is one order magnitude more difficult than Earth entry contrary to the case for grazing entry. Steep approach to that large massive planet will be troublesome.

Let us now return to the subject of aerodynamic heating. As noted earlier, at speeds exceeding Earth parabolic speed, radiation of the air in the compressed atmosphere ahead of a blunt entry body is expected to become the principal contributor to the aerodynamic heating. Thus, in contrast with the aerodynamic heating at the lower speeds where convective heating dominates so that the ratio of heat-transfer coefficient to drag coefficient can be kept small and essentially independent of the speed, the heat to drag ratio now apparently increases rapidly with increase in speed; that is to say, the fraction of the total kinetic energy per unit of vehicle mass which appears as heat to the vehicle increases with speed. But this total energy per unit of mass itself increases as the square of speed; hence, it is clear that the magnitude of the aerodynamic heating with increased speed soon reaches such alarming proportions that the fraction of vehicle mass which can be allocated to the payload becomes economically untenable.

What, if anything, can we hope to do to make more efficient entry possible at the higher speeds? This question answers itself if we but review the past developments. In the speed range of ballistic missiles, the heating during atmosphere entry was essentially all convective heating. The least ratios of heat-transfer coefficient to drag coefficient were obtained with very blunt shapes. Now for higher speed entry we must answer the question, "What shapes will provide the minimum ratio of heat-transfer to drag coefficient when both radiative and

convective heating occur and the radiative heating tends to dominate?"

The answer which has occured to me, and probably to others as well, is that we must concede some ground on convective heating if by so doing we can drastically reduce the radiative heating. To attain this end, a conical body looks attractive. As shown in figure 54–11, a conical bow shock reduces the air speed normal to the wave to $V \sin \theta_w$ in contrast to V for a severely blunt body. Of course, the drag coefficient for the conical body is less than that for the blunt body but the radiative heating should be considerably less, since it is so very speed sensitive, so that a net gain may be possible.

An analysis of this problem for entry into the Earth's atmosphere has been undertaken by my colleague Mr. Alvin Seiff and me. To date the case for the laminar boundary layer and for ablative heat shields has been completed, and it has been assumed that the conical shape is maintained during ablation—a critical assumption as will be discussed later. Some of the results to follow are most instructive. Let us define a mean value of heat-transfer coefficient, $\overline{C}_H$, so that

$$\frac{\overline{C}_H}{C_D} = \frac{\int_{-\infty}^{\infty} \frac{1}{2} C_H \rho V^3 dt}{\frac{m_E V_E^2}{2}} \tag{31}$$

The value $\overline{C}_H/C_D$ is the fraction of the total vehicle kinetic energy at atmosphere entry

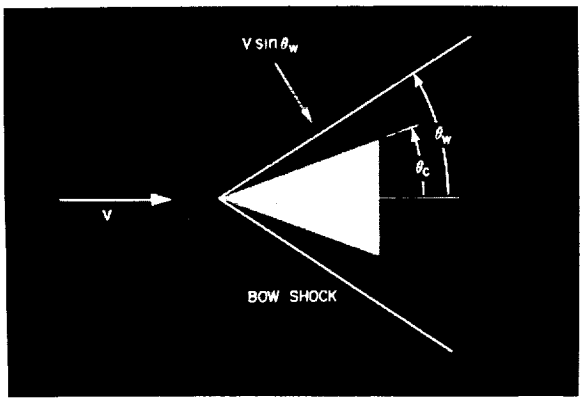

FIGURE 54–11.—Velocity vectors for conical bodies.

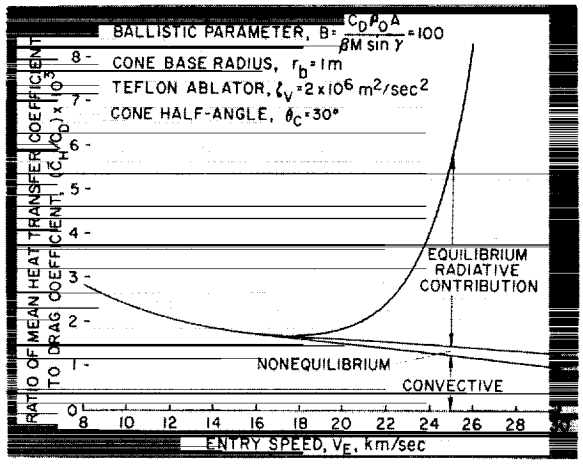

FIGURE 54–12.—Ratio of mean heat-transfer coefficient to drag coefficient for one cone half-angle.

which must appear in the form of heat to the vehicle.

It may be related directly to mass loss due to surface ablation, m_a, by

$$m_a = \frac{\overline{C}_H}{C_D \zeta_V} \left(\frac{m_E V_E^2}{2} \right) \tag{32}$$

On figure 54–12 is shown the variation of $\overline{C}_H/C_D$ as a function of entry speed for one arbitrary case in which

$$\left.\begin{array}{ll} \text{Cone half-angle;} & \theta_c = 30° \\ \text{Ballistic parameter;} & B = \dfrac{C_D \rho_0 A}{\beta m \sin \gamma} = 100 \\ \text{Cone base radius;} & r_b = 1\text{m} \\ \text{Teflon ablator, specific energy of ablation;} & \zeta_V = 2 \times 10^6 \dfrac{\text{m}^2}{\text{sec}^2} \end{array}\right\} \tag{33}$$

These particular values are not pertinent to the following discussion—rather this case should be viewed as a typical one to show the trends with speed and the contributions to the total of the convective, the nonequilibrium radiative, and the equilibrium radiative components. As seen, for entry speeds up to about 16 km/sec, the convective heating contribution dominates, indicating the very effective suppression of radiative heat transfer provided by the cone flow field. The decrease of $\overline{C}_H/C_D$ with speed in the low-speed regime is principally a

result of the effect of blowing of the ablated vapor within the boundary layer in reducing the convective transfer. When radiative heating does become important with increasing speed, it rapidly dominates. The nonequilibrium radiative contribution is relatively unimportant—a result which may be regarded as a general one.

Figure 54–13 shows the effect of varying the cone half-angle, other factors being equal. The advantage of choosing the optimum cone-angle from the envelope curve for the particular entry speed of interest is apparent. Figure 54–14 shows the envelope curves for various values of the ballistic parameter. The results shown indicate that the smallest ballistic parameter is best.

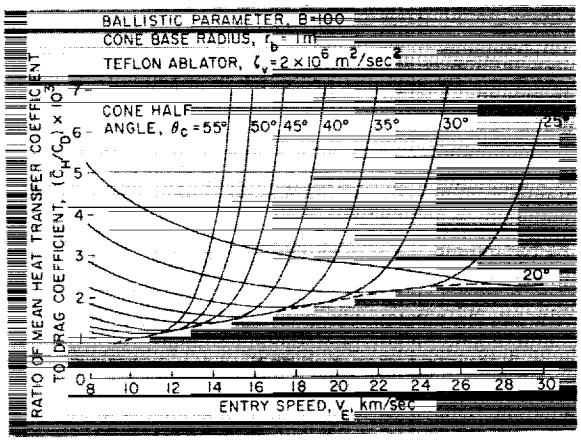

FIGURE 54–13.—Ratio of mean heat-transfer coefficient to drag coefficient as a function of cone half-angle.

However, it should be recalled that laminar flow only was assumed for these calculations and, in reality, one cannot expect to maintain laminar boundary layers to arbitrarily high Reynolds numbers. If we limit the Reynolds number to 10^7 based on local conditions—which at present seems an upper limit of what appears to be a reasonably safe value—then the least values for the ratio of mean heat transfer to drag coefficient are as indicated by the heavy solid line. The fraction of the total kinetic energy at entry to the atmosphere which must be accepted as heat energy by the heat shield can apparently be kept to low values even at entry speeds well in excess of earth parabolic speed.

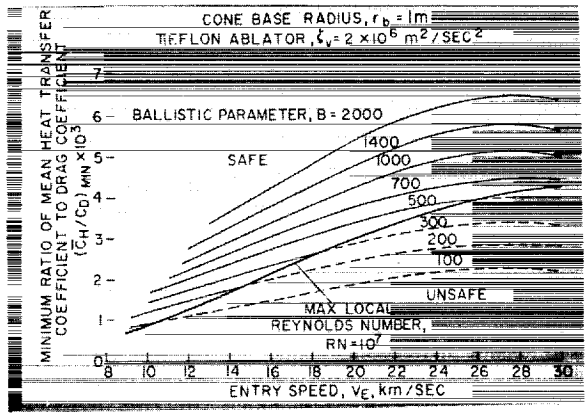

FIGURE 54–14.—Minimum ratio of mean heat-transfer coefficient to drag coefficient for various values of ballistic parameters.

Figure 54–15 gives the optimum cone half-angles as a function of speed. The optimum angles are not small even for very high entry speeds. It is of some interest to note that at the optimum condition the analysis indicates that the convective heat transfer constitutes between 85 percent and 90 percent of the total.

The corresponding ratios of ablated mass to entry mass are shown on the curve marked "Teflon ablator" in figure 54–16. It appears that one could keep the ablated mass loss to 10 percent or less to speeds up to 15 km/sec with Teflon (or equivalent ablative materials such as nylon or polyethylene). For higher entry speeds an improved ablator is needed. Graphite looks particularly appealing.

Now, it will be remembered that the foregoing analysis was predicated upon the assump-

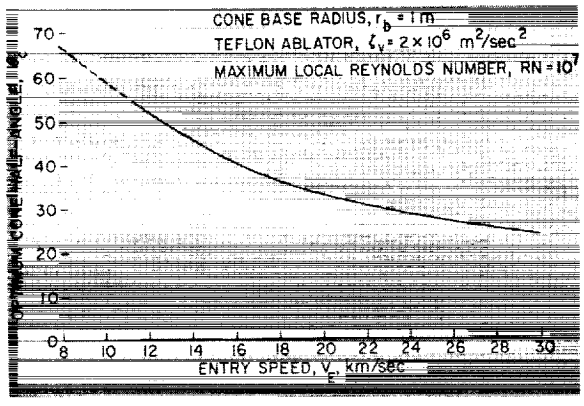

FIGURE 54–15.—Optimum cone half-angles as a function of entry speed.

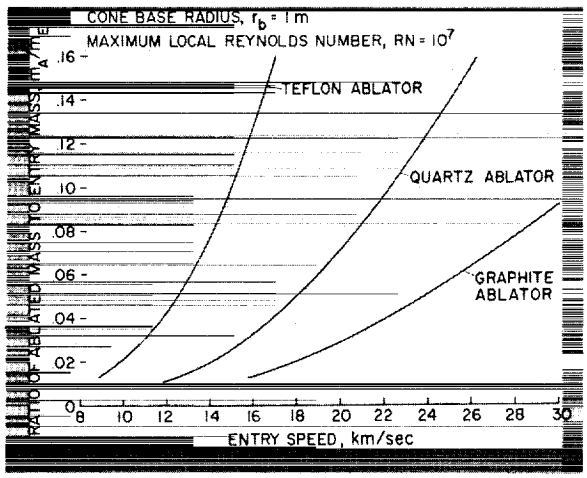

FIGURE 54–16.—Ratio of ablated mass to entry mass as a function of entry speed.

tion that the conical vehicle remained conical during entry. The local heat transfer varies greatly over the surface, being large at the cone apex and small near the base. For an ablative shield for which the heat of ablation is uniform over the surface, the ablation, accordingly, would be nonuniform over the surface. A shape which was conical at entry would become blunted by the large convective heat transfer at the apex. Then the radiative contribution would maintain this flattened forward face which would grow as the entry trajectory progressed (see ref. 23). Thus the ratio of heat-transfer coefficient to drag coefficient and, in turn, the ratio of ablated mass to entry mass would exceed those we have given previously. This increase in ablation would not be great if the entry speed were only moderately larger than Earth parabolic speed. However, it would certainly be excessive, if not overwhelming, at the highest entry speeds we have considered. The question then arises: What can be done to prevent excessive nose flattening from occurring? Several remedies suggest themselves. The more attractive of these are the following: One is to feed a solid-ablator rod (e.g., a graphite rod) of small radius through a hole at the apex at a programmed rate equal to the rate of ablation so that growth of a flattened face over the remainder of the body can be prevented. Another is to expel a suitable ablating liquid, such as water, through an orifice at the apex which could accomplish the same result. A third is to employ a near conical shape which prior to entry is cusped at the apex so as to delay the radial rate of growth of the flat face. This last alternate would probably not be as effective as the other two, but it avoids the need to program the rate of feed of ablation material. In any event it does not appear that this problem is an unsurmountable one for entry speeds up to 20 km/sec or so, but the required mass loss will exceed in some degree the amounts which were previously indicated in figure 54–16.

One final problem which, I believe, will bear investigation concerns the effects that the gas compression process in shock waves will have on the flow field about aerodynamic bodies when the enthalpy is extremely high, such as in the case for meteoric bodies, for example, at maximum entry speeds (50 to 70 km/sec for Earth). At these speeds a pointed body is blunted almost immediately. A gas cap of a blunt body, such as shown in figure 54–17(a), at the lower hypersonic speed radiates energy mostly in the long wavelength end of the spectrum. The fraction of this gas cap energy which radiates away from the body is only very minutely absorbed in the neighboring air layers ahead and to the side of the body. One can ignore, then, the effects of the radiation on the oncoming stream of air (i.e., in effect, one assumes the radiation is absorbed at infinity). As flow speed is increased, the principal radiation of the gas cap energy moves to shorter and shorter wavelengths until at very high speeds practically all the energy is radiated at such short wavelengths that a substantial fraction can be absorbed in air layers directly ahead of the body. Thus, preheating of the air ap-

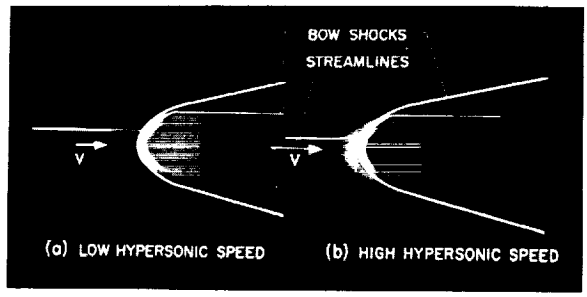

FIGURE 54–17.—Blunt bodies in hypersonic flow.

proaching the body occurs and, accordingly, the gas cap energy increases since it must accept this preheated air as the flow progresses. It appears that one effect of such "radiation trapping" is that the body must now accept more than half the energy radiated from the gas cap. Also, the air flow is no longer a usual hypersonic one since the gas ahead of the body, although moving at speed greater than that of pressure propagation, is now forewarned of the presence of the body. Moreover, the energy contained in each elemental volume can no longer be treated as constant, by virtue of the transfer of radiant energy from element to element within the flow.

Analyses concerned with prediction of temperatures and pressures within the Earth's atmosphere due to the sudden release of nuclear energy (see, e.g., ref. 24) indicate that when radiation absorption in neighboring layers becomes an important consideration, the ionization process itself brings new facets to the problem. The numerous liberated electrons, because they have a much greater mobility than the heavy particles, tend to be segregated from the main gas cap mass. Thus the flow becomes a charge-separated one so that additional flow changes are expected. In 1957, Sen and Guess (ref. 25) formulated an analysis of shock wave structure for conditions under which radiation mean free path is small and the so-called Rosseland approximation term can be used. The similar work of V. A. Prokofiev (ref. 26) is particularly enlightening. He shows that a rather dramatic thickening of the shock wave can result. To keep his mathematics and physics within bounds, Prokofiev neglected viscosity and heat conduction and treated only hydrogen and argon. His calculations, which are already rather complex, thus fail to push knowledge as far as we would like but the effects of radiation, as well as ionization, are demonstrated conclusively. My colleague, Dr. Max Heaslet, after reviewing these analyses has found that our physical knowledge has been materially improved since these earlier works appeared so that it would seem that a reanalysis is in order. He is undertaking such an analysis at this time.

However, without knowing what shock thickening is characteristic for air in very high enthalpy flows we can, in any event, describe the possible effects of such thickening. Suppose, as indicated in figure 54–17(b), the shock thickness, as indicated by the shading, becomes comparable with the dimensions of the body. The presence of the body will then be felt in the flow ahead of it by about this thickness. The stream lines will therefore resemble those we normally associate with subsonic flows, but clearly will be of a far more complex nature.

In summary, only a few of the hypersonic problems which will need solutions in the future have been treated. The advance in flight speeds and the introduction of gas media other than the air will introduce a host of new ones. Many of these requiring both analytical and experimental study are most fitting as fields of interest for our university research staffs.

REFERENCES

1. Allen, H. Julian, and Eggers, A. J., Jr.: A Study of the Motion and Aerodynamic Heating of Ballistic Missiles Entering the Earth's Atmosphere at High Supersonic Speeds. NACA Rep. 1381, 1958. (Supersedes NACA TN 4047.)
2. Gross, Joseph F., Marson, David J., and Gazley, Carl, Jr.: General Characteristics of Binary Boundary Layers With Application to Sublimation Cooling. Rand Rep. P–1371, May 8, 1958, Aug. 1, 1958 (rev.).
3. Roberts, Leonard: Stagnation-Point Shielding by Melting and Vaporization. NASA Rep. 10, 1959.
4. Lees, Lester: Convective Heat Transfer With Mass Addition and Chemical Reactions. Presented at the Third Combustion and Propulsion Colloquium, AGARD, NATO, Palermo, Sicily, Mar. 17–21, 1958.
5. Adams, Mac C.: Recent Advances in Ablation. ARS Journal, vol. 29, no. 9, Sept. 1959, pp. 625–632.
6. Chapman, Dean R.: An Approximate Analytical Method for Studying Entry Into Planetary Atmospheres. NACA TN 4276, 1958.

7. LEES, LESTER, HARTWIG, FREDERIC W., and COHEN, CLARENCE B.: The Use of Aerodynamic Lift During Entry Into the Earth's Atmosphere. Space Technology Lab. Rep. GM–TR–0165–00519, Nov. 1958.
8. EGGERS, ALFRED J.: The Possibility of a Safe Landing. Space Technology, ch. 13, Howard S. Seifert, ed., John Wiley and Sons, New York, 1959.
9. CHAPMAN, DEAN R.: An Analysis of the Corridor and Guidance Requirements for Supercircular Entry Into Planetary Atmospheres. NASA TR R–55, 1960.
10. LEVY, LIONEL L., JR.: An Approximate Analytical Method for Studying Atmosphere Entry of Vehicles With Modulated Aerodynamic Forces. NASA TN D–319, 1960.
11. KOURGANOFF, V.: Basic Methods in Transfer Problems; Radiative Equilibrium and Neutron Diffusion. Oxford, Clarendon Press, 1952.
12. UNSÖLD, ALBRECHT: Physik der Sternatmosphären, mit besonderer Berucksichtigung der Sonne. Second ed., Julius Springer (Berlin), 1955.
13. AMBARTSUMYAN, V. A., ed. Theoretical Astrophysics. Pergamon Press, New York, 1958.
14. CAMM, J. C., KIVEL, B., TAYLOR, R. L., and TEARE, J. D.: Absolute Intensity of Non-Equilibrium Radiation in Air and Stagnation Heating at High Altitudes. Avco-Everett Research Laboratory RR–93, Dec. 1959.
15. ROSE, PETER H.: Reentry From Lunar Missions. Preprint no. 7, Lunar Flight Symposium, Amer. Astronaut. Soc., Denver, Colo., Dec. 29, 1961.
16. PAGE, WILLIAM A., CANNING, THOMAS N., CRAIG, ROGER A., and STEPHENSON, JACK D.: Measurments of Thermal Radiation of Air From the Stagnation Region of Blunt Bodies Traveling at Velocities up to 31,000 Feet Per Second. NASA TM X–508, 1961.
17. KIVEL, B., and BAILEY, K.: Tables of Radiation From High Temperature Air. Avco-Everett Research Lab. RR–21, Dec. 1957.
18. MEYEROTT, R. E.: Radiation Heat Transfer to Hypersonic Vehicles. Lockheed Aircraft Corp., LMSD 2264–R1, Sept. 1958.
19. FAY, J. A., and RIDDELL, F. R.: Theory of Stagnation Point Heat Transfer in Dissociated Air. Jour. Aero. Sci., vol. 25, no. 2, Feb. 1958, pp. 73–85, 121.
20. SCALA, SINCLAIRE M., and WARREN, WALTER R.: Hypervelocity Stagnation Point Heat Transfer. General Electric Missile and Space Vehicle Dept. Rep. R61SD185, Oct. 1961.
21. HAYES, WALLACE D., and PROBSTEIN, RONALD F.: Hypersonic Flow Theory. (Applied Mathematics and Mechanics. Vol. 5.) Academic Press, New York, 1959.
22. HOWE, JOHN THOMAS: Radiation Shielding of the Stagnation Region by Transpiration of an Opaque Gas. NASA TN D–329, 1960.
23. TRIMPI, ROBERT L., GRANT, FRED C., and COHEN, NATHANIEL B.: Aerodynamic and Heating Problems of Advanced Reentry Vehicles. NASA-University Conference Report, 1962.
24. BETHE, HANS A., FUCHS, KLAUS, HIRSCHFELDER, JOSEPH O., MAGEE, JOHN L., PEIERLS, RUDOLPH E., and VON NEUMANN, JOHN: Blast Wave. Los Alamos Scientific Laboratory LA–2000, Aug. 1947, U.S. Dept. of Commerce, Washington, D.C., distributed March 1958.
25. SEN, HARI K., and GUESS, ARNOLD W.: Radiation Effects in Shock-Wave Structure. Phys. Rev., vol. 108, no. 3, Nov. 1957, pp. 560–564.
26. PROKOFIEV, V. A.: Consideration of the Effect of Emission of Radiation in the One-Dimensional, Stationary Flow of a Monatomic Gas. Uchenye Zapiski Moskovskogo Gosudarstvennogo Universieteta, Mekhanika, 172, pp. 79–124, 1952. (Translation by University Microfilms, Inc., Ann Arbor.)

666582 O—62——18

55. Recent Information on Hypersonic Flow Fields

By Alvin Seiff

ALVIN SEIFF *is chief of the Supersonic Free-Flight Wind Tunnel Branch, NASA Ames Research Center. He earned a B.S. degree from the University of Missouri in 1942 (chemical engineering). He is interested in hypersonic aerodynamics and manned space flight. Mr Seiff was associated with the development of first atomic bomb at Oak Ridge; he developed free-flight testing technique for hypersonic research; he was first to point out the effects of wall temperature on skin friction of supersonic turbulent boundary layers; he performed early studies on transition to turbulence in supersonic boundary layers; and he contributed to the development of concepts of manned lunar flight. He is an Associate Fellow of the Institute of the Aerospace Sciences. Mr. Seiff was a physics instructor at the University of Tennessee from 1946 to 1948.*

SUMMARY

This paper attempts to summarize some of the significant recent developments in the description and understanding of hypersonic flow fields. Topics discussed include the blast-wave theory, and the more exact description of pressures and bow-wave shapes to which it is applicable; Newtonian impact theory, with emphasis on its limitations; calculation of flow fields with detached bow shock waves by numerical solution of the equations of motion, with emphasis on streamtube methods; shockwave standoff distance for hemispheres as given by theory and experiment; secondary flow fields embedded within hypersonic shock layers; hypersonic flow of gases other than air; and one-dimensional shock waves with energy exchange by radiative transfer. The treatment of these topics is necessarily brief, but an effort is made to stress important conclusions, and to present references where available to permit the reader to obtain more detailed information.

INTRODUCTION

The past five years have seen some notable progress in the understanding of hypersonic gas flows. This progress has not been so much a matter of one or two brilliant discoveries but, instead, a general advancement contributed to by many investigators. The two most formidable and practically important problems of hypersonic flow—flow with a detached bow wave and the flow of real gases at elevated temperatures—have both given ground to a considerable degree. While the detailed understanding of these problems and the final description is always accomplished theoretically, the important role of experiment in defining the importance of various effects and in pointing out the existence of new effects should not be underestimated. It is significant that experimental facilities have made rapid strides within this same time period, increasing their speed capabilities by a factor of approximately 3, and now reaching speeds in the range of 36,000 to 40,000 ft/sec.

Although flow in the vicinity of a blunt nose is frequently viewed as *the* hypersonic flow problem, other problems are of interest and have received attention, including the flow field downstream of a blunt nose, such as would occur along a cylindrical surface preceded by a blunt nose, or in the wake of a blunt-nosed entry body; flow over stabilizing surfaces and controls; and flow over pointed cones. Recently, interest has developed also in the hypersonic flow of gases other than air. Several of these topics will be discussed at least briefly in this paper.

32

The theoretical methods which have been applied to these problems include some approximate methods, one of which, blast-wave theory, deserves special mention as an important first-order description of the basic hypersonic flow phenomenon, although, as will be seen, it is not quantitatively accurate at the present state of its development. The Newtonian impact theory, certainly the most widely used theory for hypersonic flow, must also be considered. A more general appreciation of the limitations of this theory is needed. Because of its simplicity, it has been somewhat wantonly applied in the recent past to problems where it is not applicable; as with any other theory, it is important to understand where the impact theory can and cannot be used.

The more exact methods of solutions applied to the blunt-body problem and to real-gas flow problems, in general, are invariably numerical solutions of the equations of motion, usually performed with an electronic computer. Although a number of techniques have been applied to obtaining these solutions, emphasis will be given to one of these, the mathematically simple stream-tube methods.

BLAST-WAVE THEORY, BOW WAVE PROFILES, AND AXIAL PRESSURE DISTRIBUTIONS

Let us begin our detailed considerations by examining the broad picture of hypersonic flow downstream of a blunt nose as given by the blast-wave theory. It will be of interest to compare this picture with experimental information and the results of more exact theory. The blast-wave theory, developed by G. I. Taylor in England and by L. I. Sedov in the U.S.S.R. (refs. 1 and 2), was originally written to consider the problem of the strong shock wave (generated, for example, by a nuclear explosion) and resulting disturbance within the wave. This problem was idealized by these authors to the case of a gas with a constant ratio of specific heats, γ, and the strong shock-wave approximations were employed. The application of blast-wave theory to hypersonic flow problems was suggested by W. Hayes, who pointed out that the radial growth of a cylindrical blast wave with time could be related to the rate of growth with distance behind the nose of the bow shock wave generated by a blunt-nosed body in hypersonic flow. The case of a cylindrical blast wave was treated in this country by S. C. Lin (ref. 3), who applied Hayes' transformation to obtain the following equations for the bow-wave profile and the axial pressure distribution for a constant $\gamma=1.4$.

$$\frac{r_s}{d}=0.80C_D{}^{1/4}\left(\frac{x}{d}\right)^{1/2} \tag{1}$$

$$\frac{p}{p_\infty}=0.0692\,\frac{C_D{}^{1/2}M_\infty{}^2}{x/d} \tag{2}$$

The first equation predicts that the bow wave will be a paraboloid of revolution. Two characteristics of this equation should be noted. One is that the bow waves described are insensitive to nose shape, depending only on the one-fourth power of the drag coefficient. Second, the equation is deficient in that the waves do not approach their known asymptotic slope, the tangent of the Mach angle, except at infinite Mach number. The second equation gives the interesting result that pressure on a cylindrical body following a blunt nose is a rapidly increasing function of Mach number, predicting, e.g., a pressure of 13.8 p_∞ at $M_\infty=20$ for a point 2 diameters behind a nose with a drag coefficient of 1. From the standpoint of the cylindrical explosion, this high pressure may be explained by saying that the energy of the explosion is at this station confined to such a cross section as to maintain the high pressure. An aerodynamicist might prefer to say that the high pressures of the nose region have carried over onto the cylinder.

The work of Sedov (ref. 2) and that of Sakurai (ref. 4 reviewed and summarized in ref. 5) indicates that the constant coefficients in Lin's equations (1) and (2), which are restricted to $\gamma=1.4$, are more properly functions of γ. These coefficients are also given in general form for any constant value of γ in reference 6.

But how accurate are these predictions? In figure 55–1 a comparison with experiment and more exact theory is shown. In figure 55–1(a) Lin's equation is compared with a correlation formula given by Van Hise (ref. 7) for a gas with constant $\gamma=1.4$. The Van Hise formula is based on a correlation of pressure distributions

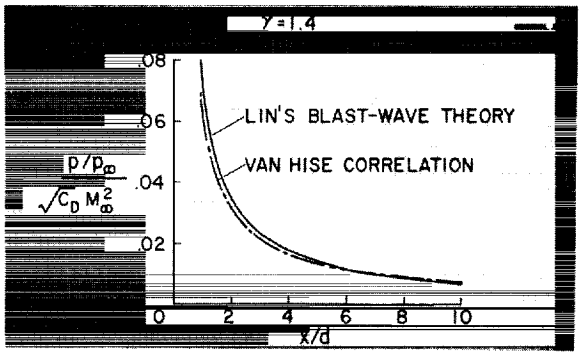

FIGURE 55–1(a).—Pressure distributions given by blast-wave theory and exact theory for very high Mach number.

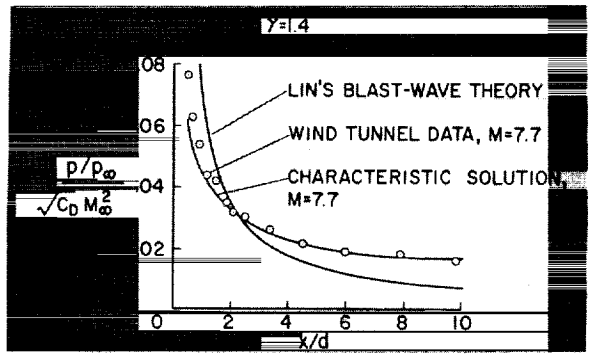

FIGURE 55–1(b).—Pressure distributions given by blast-wave theory, experiment, and exact theory at $M_\infty = 7.7$.

obtained by the method of characteristics for pointed bodies, shown in figure 55–2. The Mach numbers are for the most part, greater than 20, and the data plotted are restricted to the region beginning approximately four nose lengths downstream of the shoulder. The agreement between Lin's formula and Van Hise's correlation is exceptional. In figure 55–1(b) the blast-wave pressure distribution is compared with a wind tunnel experiment for a Mach number of 7.7 (ref. 8). While these data and the characteristics solution performed by Inouye and Lomax for the same conditions as the experiment (ref. 9) show the type of behavior called for by blast-wave theory, agreement is not quantitative. This may perhaps be a consequence of the Mach number being too low. In figure 55–1(c), the blast-wave theory is compared with a real-gas flow-field solution for a speed of 20,000 ft/sec (ref. 10). Again, agreement is only qualitative, perhaps because of a violation of the assumption of constant $\gamma = 1.4$. This is a representative current picture of comparisons of the blast-wave pressure distribution with experiment and more exact theory—it is qualitatively correct, but quantitatively frequently in appreciable error. The basic description of the flow field provided by blast-wave theory is correct, however, to a first order of approximation, and the validity of the view that the blunt-nosed body at hypersonic speed may be considered as a cylindrical explosion phenomenon is confirmed.

Also shown in figure 55–1(c) is a predicted bow wave compared with an experimental bow wave at a Mach number of 15. About the same type of comparison is obtained as in the case of the pressure distributions. If the waves are made to start at the same origin, the theoretical wave intersects and passes through positions

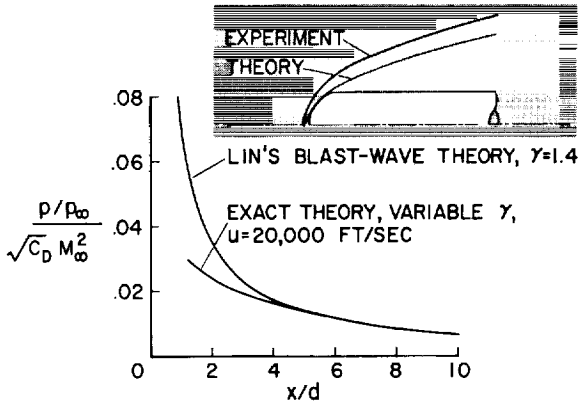

FIGURE 55–1(c).—Pressure distributions given by blast-wave theory and exact theory for real air.

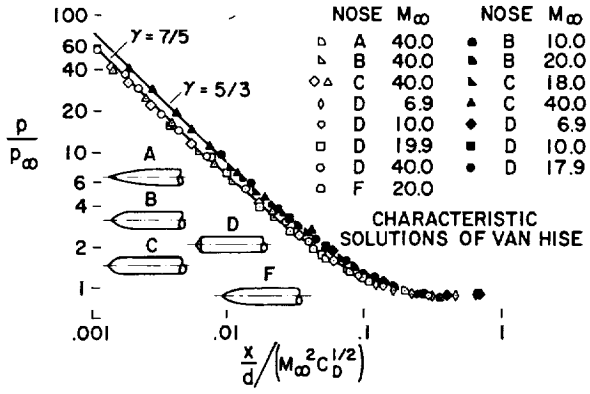

FIGURE 55–2.—Correlation of body-surface pressures by use of blast-wave variables.

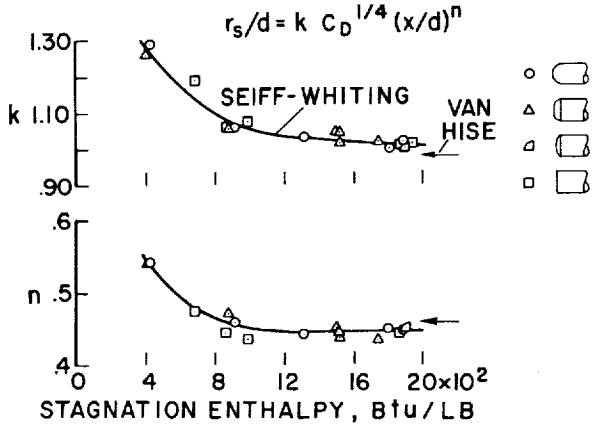

FIGURE 55–3.—Correlation of bow-wave profiles by use of blast-wave variables.

occupied by the body, which is clearly impossible. However, it is found that the form indicated by blast-wave theory for the wave equation is very suitable for describing experimental shock waves, with only minor alterations in the coefficients and exponents. The latter can, in fact, be correlated as a function of a stream total enthalpy (ref. 11). Such a correlation is shown in figure 55–3. It is particularly noteworthy that the one-fourth power dependence on drag coefficient successfully brings together data from the set of blunt noses shown in the figure, which show appreciable variations in both wave profile and drag coefficient. Although the exponents and the coefficients obtained differ importantly from the theoretical values for quantitative purposes, they are of the theoretical magnitude.

The above correlations are restricted to the region "not too close" to the body nose. In the nose region, as noted above the hemispheres, the theoretical bow wave intersects and passes through the body nose. Experimentally, the wave profile in the nose region is smooth and continuous and never intersects the surface. A detailed comparison of the blast-wave shock profile and some experimental nose-region profiles is shown in figure 55–4 for a pair of highly blunt noses. Since the experimental bow-wave profiles necessarily lie outside the theoretical, it may be said that the wave growth in this region is forced by the nose profile, rather than being allowed to take the "natural" growth curve of a cylindrical blast wave.

It is interesting that a two-line fit to the shock-wave coordinate data on logarithmic paper yields a very adequate description of the wave ordinates in this figure (ref. 11). The nose-region power law expression for the bow wave has a smaller exponent than that for the downstream region. The exponent tends to be further reduced by decreasing the shock-wave standoff distance. This may be interpreted as an approach to a step wave, for which the exponent would be zero. Where the theory is violated as a result of the nose forcing the rate of wave growth, the pressures predicted must also be in error and only become valid 2 or 3 diameters downstream.

In the region to which blast-wave theory may be applied, the following technique has been used to obtain the flow-field properties throughout the disturbed flow with considerably improved accuracy over blast-wave theory (ref. 12). The bow-wave profile is taken from the correlations described by figure 55–3. A pressure distribution in the radial direction mathematically similar to that given by blast-wave theory is assumed. The value of the static pressure at the bow wave is calculated from the wave slope, and the body surface pressure is determined from a numerical integration to satisfy continuity of flow through the cross section considered. This technique is comparatively easy to apply and has in some cases led to excellent agreement with the results of more exact calculations, as shown in figure 55–5. The profiles of density, temperature, and velocity ob-

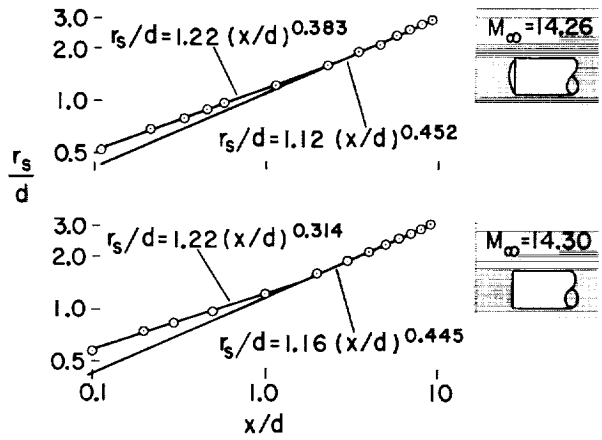

FIGURE 55–4.—Relation of nose region and downstream bow waves of very blunt bodies.

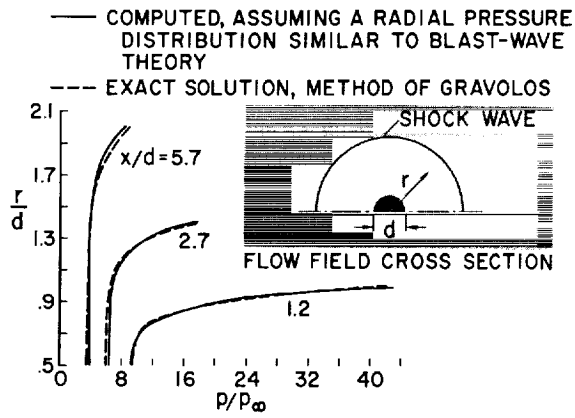

FIGURE 55–5.—Improvement of the blast-wave solution by use of correlated experimental shock wave.

tained in this case are in as good agreement with exact theory (from ref. 10) as the pressure profiles shown. It should be expected, however, that whenever the form of the pressure distribution in the cross section differs from that given by blast-wave theory, the accuracy of the computed properties would deteriorate.

FLOW IN THE NOSE REGION OF BLUNT-NOSED BODIES

Limitations of Newtonian Impact Theory

Turning now to consideration of the flow in the nose region of blunt-nosed bodies, we may begin by noting that this is the problem to which the Newtonian impact theory most properly applies. The flow described by impact theory is one in which the component of free-stream momentum normal to the body surface is lost while the component parallel to the surface is unchanged. This condition is most nearly realized in a thin disturbance layer where the flow direction is of necessity approximately parallel to the body surface. Since the predominant mechanism for altering the free-stream momentum is the bow shock wave, which for a thin disturbance layer is approximately parallel to the surface, and since it is a known property of oblique shock waves that the component of velocity parallel to the wave is unaffected by the wave, the basic conditions for impact flow obtain when the shock or disturbance layer is thin. A corollary to this statement is that the basic conditions for impact flow are not satisfied unless the shock layer is locally thin and the shock wave approximately parallel to the body surface, since it cannot then be assumed that the component of momentum parallel to the surface is the same as that in the free stream.

It has long been recognized that a thin shock layer is not necessarily a uniform pressure layer normal to the body surface, since curvature of the surface dictates that the streamlines be curved and that pressure gradient exist normal to the flow direction. For convex surfaces, the pressure immediately behind the shock wave must be higher than that at the body surface. Early investigators tried to define a centrifugal-force correction to be applied to the impact theory (see, e.g., ref. 13). However, it is not correct to assume that the impact theory gives the pressure immediately behind the shock wave, for two basic reasons: (1) The shock-wave angle is, in general, greater than the body surface angle at corresponding points; and (2) even if the wave angle rather than the body angle were used in the impact pressure equation, the pressure coefficient would be in error by a factor $1-\rho_\infty/\rho_2$ because the momentum normal to the wave is not entirely lost at the wave. Thus, an essential shortcoming of centrifugal-force corrections is that the pressure to be corrected, that immediately behind the shock wave, is not obtained from simple impact theory. Experience has shown that these corrections are not in general successful, and the simple impact theory is to be preferred over the corrected theories. Furthermore, detailed investigations made by more exact theories show that the pressure differences from the body to the shock wave are not usually as large as 20 percent of the body surface pressure.

The impact theory equation for pressure coefficient, $C_p=2\ (\sin\theta)^2$, is now ordinarily modified by replacing the coefficient 2 by the pitot pressure coefficient C_{pt} to obtain $C_p=C_{pt}\ (\sin\theta)^2$. The latter form, conventionally referred to as modified Newtonian theory, insures that the pressures will be correct at and in the vicinity of the flow stagnation point.

Even in the case of the blunt-nosed body, conditions arise in which the impact theory fails

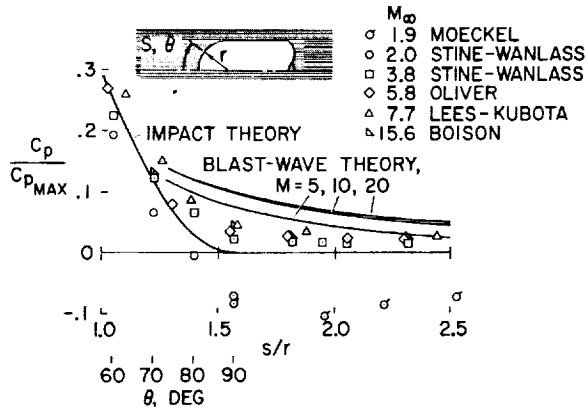

FIGURE 55-6(a).—Deviation from impact theory of pressures near the base of hemispheres.

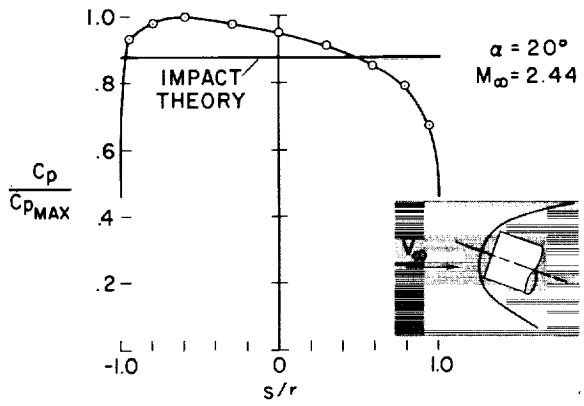

FIGURE 55-6(b).—Deviation from impact theory of pressures on a flat face at angle of attack.

to give the pressure distribution accurately. Two of these are illustrated in figure 55–6. (Experimental data in this figure are from refs. 8 and 14 through 17.) The first is the case of a hemisphere cylinder at high Mach number. The modified impact theory, which is by definition exact at the stagnation point, gives the pressure distribution correctly to at least 45° surface angle from the stagnation point. At the higher angles shown in the left part of this figure, and on the cylindrical afterbody, the errors of the theory, expressed as percent of the measured pressures, become large. A deviation of the data from the theory obviously means that the theoretical assumptions are not being met. The shock wave at these stations is departing from parallel to the surface and is gradually moving away, just as the pressures are gradually beginning to disagree. It is interesting to see how the region of the impact theory, the nose region, gives way to the region of the blastwave theory as the experimental data make a transition from one to the other. As the Mach number is increased, the level of pressures on the back part of the hemisphere tends to increase. The impact theory does not, then, give the high Mach number limit of the pressure distribution on a hemisphere.

For the region of departure of the pressure data from impact theory, it has been observed by Lees and Kubtoa (ref. 8) that Prandtl-Meyer expansion equations relating stream angle to pressure can be used to estimate the pressures.

The second example in figure 55-6(b) is of interest and importance to entry vehicles which, like the Mercury and Apollo, have essentially flat faces. The impact theory predicts for this case a uniform pressure over the face, as shown. Experiment (unpublished wind-tunnel measurements by Stalder and Seiff) shows an appreciable variation in pressure, which is maximum near the leading corner, as might be expected intuitively. This failure of the theory is again attributable to an inadequate description of the shock wave, which should ideally be plane and parallel to the face. A more realistic shock-wave profile is shown sketched. It is interesting that the eccentricity of the experimental pressure distribution is responsible for a thin disk being statistically stable in flight with its flat face normal to the flight direction.

More Exact Theory

Since the impact theory is unfortunately unable to quantitatively describe in all cases the flow over a blunt nose, more exact theories are required. Certainly, fundamental interest in such flows also leads to more detailed investigations. This problem has attracted much interest and attention in the last 10 years, and a number of methods of attack have been described and applied. These have been well summarized in the textbook on Hypersonic Flow Theory by Hayes and Probstein (ref. 6), and it will not be the purpose of the present paper to repeat this summary. The writer would, however, like to indicate what in his opinion is

the present state of this field of investigation, and to point out some of the significant developments.

It is important to note, for example, that all presently available solutions which may be referred to as exact are numerical solutions, rather than explicit functional solutions, for the flow variables. Also, the methods of solution may be classified in three groups: (1) those that seek to integrate the complete equations of motion, given the body shape; (2) those that specify a shock shape and numerically integrate the equations of motion to define the flow field and the body shape; and (3) the so-called stream-tube methods. The first group considers perhaps the most difficult problem. One of the essential boundaries of the flow, the shock wave, is initially unknown in shape and position. Computational difficulties arise near the sonic line, and the computations are, in general, quite complex and intricate. Accordingly, very few solutions by these techniques have been published. The second group, by specifying the shock wave, and finding the body shape as a result of the computation, raises the objection that one cannot directly solve the problem of a particular body shape which may be of immediate interest. Also, for certain ranges of conditions, the body shape is very sensitive to small changes in the shock-wave shape. This is particularly true for nearly flat faced bodies. Computational difficulties initially associated with this approach have been overcome at least for the case of the ideal gas (refs. 18 and 19).

The third method, the stream-tube method, has an essential simplicity which is at once appealing and surprising—surprising because the inherent difficulty of the blunt-body problem has become almost an axiom of our time. The principles which must be understood to apply the stream-tube method are elementary. The method is, like the others, somewhat laborious and requires iteration. It also runs into numerical accuracy difficulties for the nearly flat body, which apparently poses problems for all known methods of solution.

In the stream-tube method (see fig. 55–7), one-dimensional flow equations are applied to the individual stream tubes and the following assumptions are made:

$$(r_b + y_s \cos\theta)^2 = 2y_s^2 \int_0^1 \frac{\rho}{\rho_\infty}\frac{u}{u_\infty}(\cos\alpha)\left(\frac{r_b}{y_s} + \frac{y}{y_s}\cos\theta\right) d\frac{y}{y_s}$$

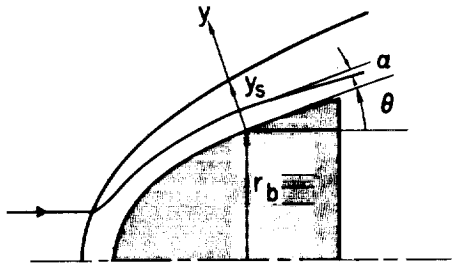

FIGURE 55–7.—Stream-tube method.

(1) The flow in each stream tube is isentropic downstream of the bow wave and has the entropy determined by the free-stream conditions and the shock-wave angle where the stream tube crosses the bow shock wave.

(2) The total enthalpy in each stream tube is a constant and equal to the free-stream total enthalpy.

(3) The pressure gradient normal to the stream tube is determined by the stream-tube curvature and is given by $\frac{\partial p}{\partial y} = \frac{\rho u^2}{R}$.

The Rankine-Hugoniot equations are applied at the bow wave to determine conditions immediately behind the wave. An equation of state, which for a real gas may take the form of a Mollier diagram or other graphical or tabular presentation of the relationship between the state variables, is also required.

Solutions are found at a preselected number of stations along the body surface, such as the one indicated in figure 55–7. The procedure is iterative and begins with a first approximation to the surface pressure distribution and the bow-wave shape and standoff distance. The assumed bow wave and pressure distribution are improved in successive iterations until a completely consistent set of values is obtained. The next approximation to the shock-wave contour is obtained by determining its normal distance from the body surface at each station and connecting the points so obtained. The normal distance of the shock wave from the surface must

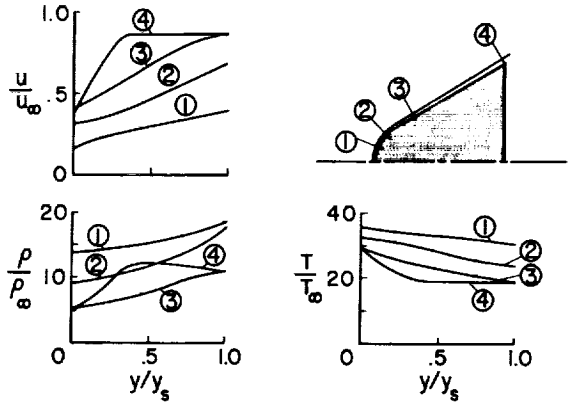

FIGURE 55–8.—Flow field computed by stream-tube method; μ_∞ =33,000 ft/sec; altitude=171,500 ft.

be that required to satisfy continuity of flow through the station under consideration, according to the equation shown in figure 55–7.

Solutions have been obtained by this method, with some minor variations, by a number of authors, including Maslen and Moeckel (ref. 20) and Gravalos, Edelfelt, and Emmons (ref. 21). One which has not been previously published by the present author is shown in figure 55–8, for a round-nosed 30° half-angle cone at a flight velocity of 33,000 ft/sec and an altitude of 171,500 feet. The shock-wave position and shape shown in the figure are drawn approximately to scale. In obtaining this solution, the cosine of the streamline inclination to the surface was taken equal to 1, and two iterations were performed to obtain a good approximation to the final shock shape. The state properties of real air at equilibrium were employed. Results of interest include the extreme thinness of the shock layer over the entire surface; the comparatively large variations within this thin layer of velocity, temperature, and density resulting from bow-wave curvature over the spherical nose; and the correspondence of flow properties in the outer part of the flow over the conical surface to pure conical flow properties at the same flight conditions.

Three-dimensional hypersonic blunt-body flows, such as those over spherical segment noses at angle of attack, have also been studied by use of stream-tube methods. Additional assumptions employed in reference 22 for this case include the following: (1) The bow shock wave is made up of circular arc segments, meeting in tangent intersection at the point where the shock wave is perpendicular to the stream; (2) The surface streamlines are radial to the stagnation point; and (3) The average mass flow per unit area at a given station is the average of the values at the bow wave and the body surface. With these assumptions, solutions are obtained which compare closely enough with experimental observations to be considered very useful.

Shock-Wave Standoff Distance

A quantity which has frequently been used for comparison of various theories and for comparing theories with experiment is the shock-wave standoff distance at the stagnation point, since a good quality schlieren or shadowgraph picture provides this information. The standoff distance also has practical importance for radiative heat transfer from the gas to the surface, since it determines the volume of gas available to radiate. It is now well known that the standoff distance is determined by mass conservation considerations, since, as was discussed in connection with the stream-tube methods of flow analysis, the mass flow passing between the body surface and the bow wave at any given station must match that crossing the bow wave inside that station. The principal variable affecting the mass flow ratio, $\rho_1 u_1/\rho_\infty u_\infty$, is the gas density ratio, ρ_1/ρ_∞, since the velocity ratio is at high speeds relatively unaffected by speed, dissociation, etc. Hence, the shock-wave standoff distance for any given configuration is correlated in terms of the density ratio across the shock wave on the stagnation streamline. This type of correlation and a comparison of various theories and experiments is shown in figure 55–9 for hemispherical noses. It can be seen that the experimental points, from references 23, 24, and 19, and exact theoretical points, from references 19 and 25, define a dependence of standoff distance on density ratio that is essentially independent of other test variables. An approximate theory of Serbin (ref. 26) that fits the more exact theories very well has been included. The experimental data are observed to scatter somewhat more than do the various theories. This scatter can probably be attrib-

uted to two principal causes—light refraction effects distorting the body position, and failure of the flow to obtain complete chemical and thermodynamic equilibrium, particularly at the lower density ratios. The Van Dyke theoretical points are for a series of Mach numbers, increasing toward the origin. The Wick-Kaattari line is also for a range of flight conditions extending approximately up to the escape speed from earth. The Seiff point is from the solution figure 58–8. In the range of density ratio from 0 to 0.2, these collected data can be very well represented by the linear equation, $\delta/R_n = 0.78\ \rho_\infty/\rho_1$. According to reference 25, this figure is applicable not only to complete hemispheres but also to spherical segments with arc half angles greater than about 39°.

It is important to note that shock waves in monatomic gases, such as helium, are limited to density ratios greater than 0.25, which is the density ratio for a normal shock wave in ideal air at a Mach number of 3.16. Hence, the bow shock wave in helium tests will never approach closer to the body than it does in air at a Mach number of 3.16.

Shock-wave angles in cone flow are analogous to shock-wave standoff distances in blunt-body flow. It is appropriate to refer to the angle between the bow wave and the surface as the shock-wave standoff angle. This angle is determined by mass flow considerations and may be estimated on this basis (ref. 27).

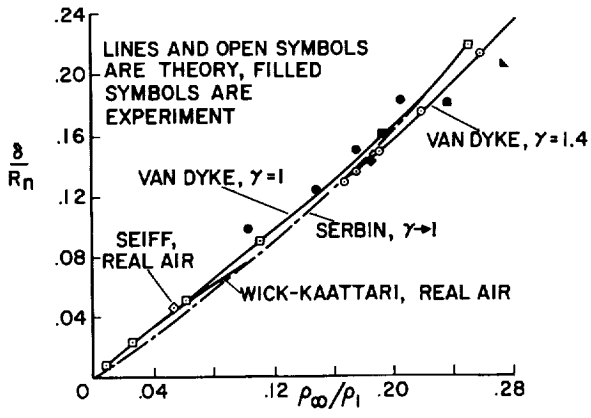

FIGURE 55–9.—Correlation of shock wave standoff distance with density ratio at the shock wave for spheres.

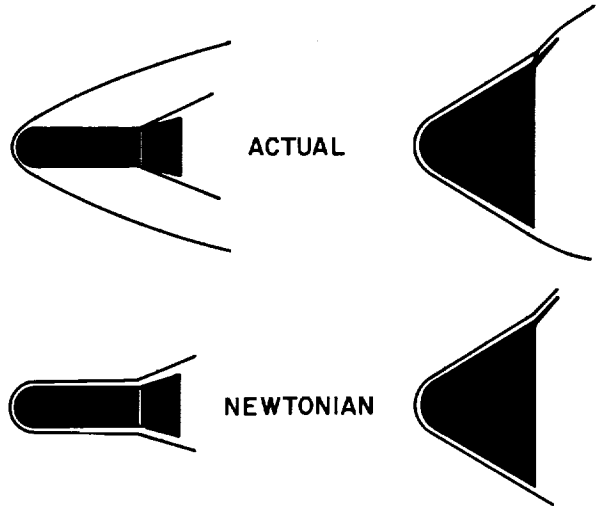

FIGURE 55–10.—Hypersonic flow configurations.

THREE FURTHER TOPICS

Embedded Flows

Most early considerations of hypersonic flow did not include within their scope complex effects such as are conventionally considered in airplane design including wing-body interference. However, it is now clear that such effects can and do arise. It is particularly necessary to consider the flow-field interference when an aerodynamic element, such as a stabilizer or control, is located in a supersonic region of a hypersonic disturbance field. Two examples of such flows are indicated schematically in figure 55–10. The flow configuration, as it is now known, is shown in the upper part of the figure, while that predicted according to impact theory is shown in the lower part. On the left, two differences between the flow configurations may be noted: (1) The degree to which the bow shock wave confines the disturbed flow to a thin layer is far less for the actual flow than the Newtonian, and (2) since the flow approaching the stabilizer is supersonic, it generates a secondary shock wave, an embedded flow field. On the right, the actual bow shock wave meets the requirements for Newtonian flow, but since the surface Mach number at the base is supersonic, again, an embedded shock wave occurs on the flap.

The existence of the embedded flow field clearly indicates that the pressures on the de-

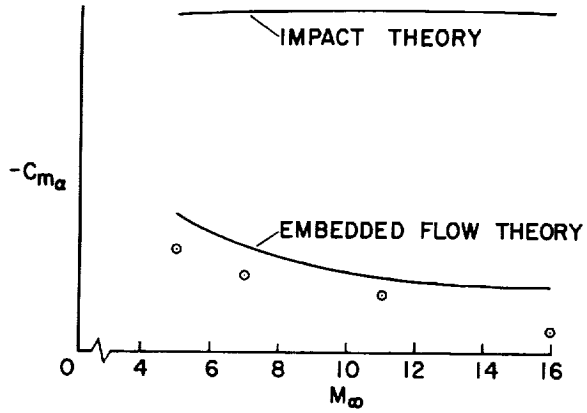

FIGURE 55–11.—Hypersonic flight stability of blunt-nosed flare-stabilized bodies.

flected surface must be analyzed in terms of the local conditions ahead of that surface. In reference 28, the use of a Newtonian approximation based on local flow conditions ahead of the flare or flap is proposed. Available data show that the accuracy obtained by this approach is about the same as the Newtonian theory normally obtains when applied to usual blunt-body problems. This type of calculation can be used to estimate pressures, normal force, and stability.

The interactions under discussion produce some large and surprising effects. For example, in the case of bodies like those shown at the left in figure 55–10, stability variations with Mach number occur in the hypersonic range, where it has conventionally been assumed that Mach number effects would not occur. One example of this is shown in figure 55–11. A comparison of the measured stability with impact theory and with embedded flow theory shows that impact theory is grossly in error, while the embedded impact flow model gives a reasonable approximation to the stability. In the case of the flap problem shown by the sketches on the right in figure 55–10, the effects obtained are illustrated in figure 55–12. A large variation in surface pressure on the flap with distance from its leading edge is calculated to result from variations in local flow variables through the shear layer on the parent body presented in figure 55–8. Surface pressure coefficients approach 5 compared to the Newtonian maximum of 2, because of the more efficient compression process utilizing two shock waves of lower strength rather than the single strong shock-wave process. As is well known, isentropic compression of the free stream would yield pressure coefficients in the hundreds and thousands at hypersonic speeds. A comparison of figures 55–11 and 55–12 shows that in one case, Newtonian theory overestimates the pressures, and in the other case, underestimates them. In both cases, the errors are serious.

With the impact flow model, the effects under present consideration would not occur. The question may legitimately be asked, "Would these flow configurations tend to go to the Newtonian limit at sufficiently high speed?" The answer, as the present writer sees it, is no. Both from empirical observations and from the theoretical arguments of Oswatitsch (ref. 29), it is known that the distribution of local Mach numbers in the flow field becomes invariant with Mach number at high supersonic speeds. Hence, a locally supersonic Mach number will remain locally supersonic, and it follows that a concave corner will generate an embedded shock wave at all flight speeds, however high. Also, in light of the blast-wave theory, the bow-wave configuration shown in the upper left of figure 55–10 will continue to be the type of wave configuration at indefinitely high speed, although it may tend to approach the body somewhat as gaseous dissociation becomes complete behind the shock wave and ionization becomes appreciable, both of which effectively lower the ratio of specific heats. For conditions where the principal bow wave intersects the flap or control, Newtonian flow may be obtained on the flap in the outer portions.

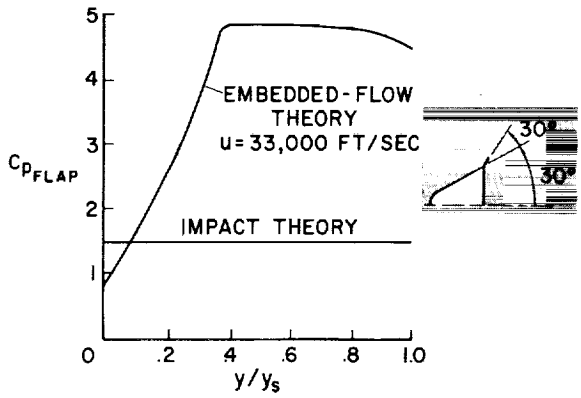

FIGURE 55–12.—Embedded flow on a flap control.

Flows in Other Gases

Most recently, interest has developed in gas flows involving gases other than air. This is stimulated by (1) a desire to use test gases which do not liquefy when expanded to high Mach numbers, such as helium, and (2) interest in entries into the atmospheres of the planets Mars and Venus which atmospheres are usually assumed to consist predominantly of mixtures of nitrogen and carbon dioxide.[1] The importance of the gas composition depends on which flow-field properties are under consideration and on the body shape. For cases where the Newtonian approximation is valid, pressure distribution and force produced will not depend significantly on the gas employed, since Newtonian pressure equation is independent of all gas characteristics. It may be noted, however, that air flows will tend to approach the Newtonian condition more closely than helium flows because of the thinner shock layers in air.

It has also been shown that air and helium flow will differ systematically in the regime where blast-wave theory applies, on cylinders behind blunt noses. It can be seen in figure 55–2 that afterbody pressures behind blunt noses are 10 to 15 percent higher in helium than in air, and it is also found (ref. 7) that the bow-wave radius of cross section is roughly 5 percent greater in helium than in air.

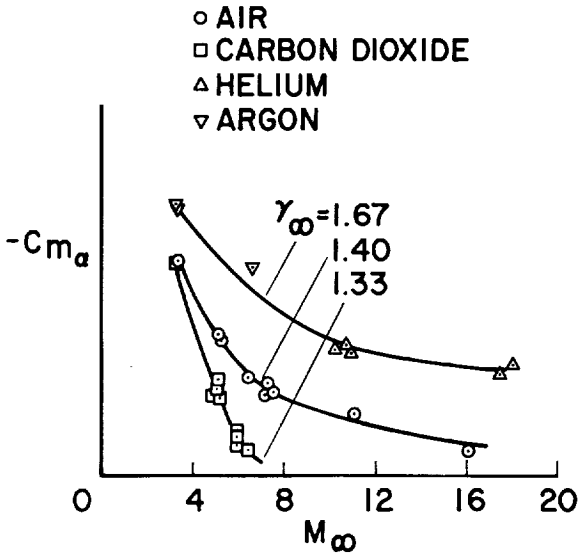

FIGURE 55–13.—Flight stability of in four gases of a a blunt-nosed flare-stabilized body.

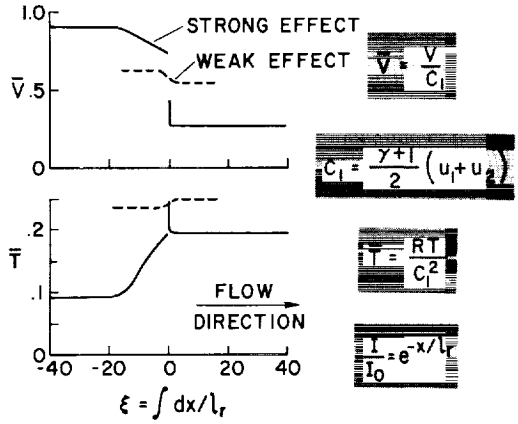

FIGURE 55–14.—Normal shock wave with radiative energy exchange.

Configurations which generate embedded flow fields will apparently be especially sensitive to gas composition. This is shown in figure 55–13 by a collection of data from reference 30 for a flare-stabilized blunt-nosed body. These effects on static stability are surprisingly large. They are predictable as to trend, at least, by the same method employed in the preceding figure. These results give indication of interesting problems yet to come in the gas dynamics of other gas mixtures.

Flow With Radiative Energy Exchange

A classical assumption of gas dynamics has been the assumption of constant energy on streamlines outside of the boundary layer. The consideration of gases which are luminescent as a result of compression processes in the flow field has brought a realization that energy exchange must be allowed. Normally, one thinks first of energy loss by radiation from the high temperature gases near a stagnation point. There will, of course, also be regions of the flow for which there is a net gain in energy by radiation absorption. This is true, for example, of the gas immediately ahead of a strong shock wave.

These problems have been considered in references 31 and 32 and are also the subject of a recent study by Heaslet and Baldwin at Ames Research Center. Some results from their study are shown in figure 55–14. The problem

considered was the one-dimensional normal shock wave in a radiating and absorbing gas. Distributions of temperature and velocity, in dimensionless form, are shown as a function of dimensionless distance in the flow direction. The physical coordinate, $d\bar{x}$, is divided by the local mean free path for absorption and integrated to obtain ξ. Two cases are shown, a weak effect, corresponding to a weak shock wave and low radiation levels, and a strong effect, corresponding to a strong shock wave and high radiation levels. The weak effect case shows a spreading out of the shock wave so that no discontinuous jump occurs in velocity or temperature. The shock wave is diffused over a distance of about four radiation mean free paths. This is analogous to the effects of viscosity or thermal conductivity in diffusing the shock surface. In the strong effect situation, the velocity shows a definite discontinuity, but also shows an upstream influence due to radiation ahead of the shock wave to a distance of about 20 mean free paths of the radiation. The temperature distribution also shows a discontinuity—an adiabatic, inviscid shock wave—and a very local overshoot jump immediately behind the wave. Although the overshoot resembles a relaxation-induced effect, nonequilibrium conditions were not included in this study, so the overshoot is purely a result of the radiative energy exchange. The over-all temperature and velocity changes obey the Rankine-Hugoniot equations and hence match the corresponding values for the case of no radiative energy exchange. Further studies in flows with radiative energy exchange will certainly be of interest and importance at very high flight speeds.

CONCLUDING REMARKS

In this review, we have attempted to touch on some of the significant quantitative results available pertaining to hypersonic flow fields. Needless to say, it has not been possible within this brief note to describe in sufficient detail all of the important work which has been done, and some very interesting and competent investigations have had to be dismissed with just a few words. Much useful quantitative work has been done within the last 10 years. In fact, it is true that most of today's quantitative knowledge of hypersonic flow is a product of that period.

It is somewhat of a gamble to try to predict what direction future work should or will take. One thing is certain, consideration will be given to still higher flight speeds. The phenomenon of departure from adiabatic flow has been mentioned as a future problem area. The characteristics of highly ionized flow fields will also have to be considered and evaluated. A problem that is receiving attention, but still has not been resolved to a few simple conclusions, is that of flow with nonequilibrium chemistry and thermodynamics, which tends to occur at high flight altitudes. In addition, a practically endless set of questions awaits us in the study of the dynamics of gases other than air. It seems that the next 10 years can easily be as interesting and as challenging as the 10 years just past.

SYMBOLS

C_D	drag coefficient
C_p	pressure coefficient, $\frac{p-p_\infty}{q_\infty}$
C_{m_α}	static stability coefficient
d	body diameter
M	Mach number
p	pressure
q	dynamic pressure, $\frac{1}{2}\rho u^2$
r	radius of cross section
R	radius of curvature
s	distance along surface from stagnation point
T	temperature
u	air velocity
x	axial coordinate
y	coordinate normal to body surface
α	angle of attack, or angle between streamline and body surface (fig. 55–7)
δ	shock-wave standoff distance at stagnation point
γ	adiabatic exponent, ratio of specific heats
ρ	air density
θ	surface angle relative to free stream direction
ξ	dimensionless coordinate in flow direction, figure 55–14

Subscripts:

∞	in the undisturbed free stream
1	behind the bow shock wave
b	body
n	body nose
s	at the shock wave
t	total

REFERENCES

1. TAYLOR, GEOFFREY: The Formation of a Blast Wave by a Very Intense Explosion. Proc. Roy. Soc. London. Ser. A, vol. 201, no. 1065, 1950, pp. 159–186.
2. SEDOV, L. I. (Maurice Holt, ed., trans.): Similarity and Dimensional Methods in Mechanics. Gostekhizdat, SSSR. Third ed. 1954, fourth ed. 1957. Academic Press (New York), 1959.
3. LIN, S. C.: Cylindrical Shock Waves Produced by Instantaneous Energy Release. Jour. Appl. Phys., vol. 25, no. 1, 1954, pp. 54–57.
4. SAKURAI, A.: On the Propagation and Structure of the Blast Wave. I. Jour. Phys. Soc. Japan, vol. 8, 1953, pp. 662–669. II. Jour. Phys. Soc. Japan, vol. 9, 1954, pp. 256–266.
5. LUKASIEWICZ, J.: Hypersonic Flow-Blast Analogy. AEDC–TR–61–4,, Arnold Engineering Development Center, Air Force Systems Command, June 1961.
6. HAYES, WALLACE D., and PROBSTEIN, RONALD F.: Hypersonic Flow Theory. Academic Press (New York), 1959.
7. VAN HISE, VERNON: Analytic Study of Induced Pressure on Long Bodies of Revolution With Varying Nose Bluntness at Hypersonic Speeds. NASA TR R–78, 1961.
8. LEES, LESTER, and KUBOTA, TOSHI: Inviscid Hypersonic Flow Over Blunt-Nosed Slender Bodies. Jour. Aero. Sci., vol. 24, no. 3, March 1957, pp. 195–202.
9. INOUYE, MAMORU, and LOMAX, HARVARD: Comparison of Experimental and Numerical Results for the Flow of a Perfect Gas About Blunt-Nosed Bodies. NASA TN D–1426, 1962.
10. FITZGIBBON, SHEILA: Lines of Constant Pressure, Density, and Temperature for Real Gas in the Supersonic Flow Field About a Hemisphere-Cylinder. Program Information Release 116–248, General Electric Co., Aug. 1960.
11. SEIFF, ALVIN, and WHITING, ELLIS E.: A Correlation Study of the Bow-Wave Profiles of Blunt Bodies. NASA TN D–1148, 1962.
12. SEIFF, ALVIN, and WHITING, ELLIS E.: Calculation of Flow Field From Bow-Wave Profiles for the Downstream Region of Blunt-Nosed Circular Cylinders in Axial Hypersonic Flight. NASA TN D–1147, 1961.
13. GRIMMINGER, G., WILLIAMS, E. P., and YOUNG, G. B. W.: Lift on Inclined Bodies of Revolution in Hypersonic Flow. Jour. Aero. Sci., vol. 17, no. 11, Nov. 1950, pp. 675–690.
14. MOECKEL, W. E.: Experimental Investigation of Supersonic Flow With Detached Shock Waves for Mach Numbers Between 1.8 and 2.9. NACA RM E50D05, 1950.
15. STINE, HOWARD A., and WANLASS, KENT: Theoretical and Experimental Investigation of Aerodynamic-Heating and Isothermal Heat-Transfer Parameters on a Hemispherical Nose With Laminar Boundary Layer at Supersonic Mach Numbers. NACA TN 3344, 1954.
16. OLIVER, R. E.: An Experimental Investigation of Flow Over Simple Blunt Bodies at a Nominal Mach Number of 5.8. CIT MEMO no. 26, June 1955.
17. BOISON, J. CHRISTOPHER: Experimental Investigation of the Hemisphere-Cylinder at Hypervelocities in Air. AEDC–TR–58–20, Arnold Engineering Development Center, Air Research and Development Command, Nov. 1958.
18. VAN DYKE, MILTON D.: The Supersonic Blunt-Body Problem—Review and Extension. Jour. Aero/Space Sci., vol. 25, no. 8, Aug. 1958, pp. 485–496.
19. VAN DYKE, MILTON D., and GORDON, HELEN D.: Supersonic Flow Past a Family of Blunt Axisymmetric Bodies. NASA TR R–1, 1959.
20. MASLEN, S. H., and MOECKEL, W. E.: Inviscid Hypersonic Flow Past Blunt Bodies. Jour. Aero. Sci., vol. 24, no. 9, Sept. 1957, pp. 683–693.
21. GRAVALOS, F. G., EDELFELT, I. H. and EMMONS, H. W.: The Supersonic Flow About a Blunt Body of Revolution for Gases at Chemical Equilibrium. TIS R58SD245, General Electric Missile and Space Vehicle Dept., June 1958.
22. KAATTARI, GEORGE E.: Predicted Shock Envelopes About Two Types of Vehicles at Large Angles of Attack. NASA TN D–860, 1961.
23. SEIFF, ALVIN, SOMNER, SIMON C., and CANNING, THOMAS N.: Some Experiments at High Supersonic Speeds on the Aerodynamic and Boundary-Layer Transition Characteristics of High-Drag Bodies of Revolution. NACA RM A56105, 1957.

24. PAGE, WILLIAM A., CANNING, THOMAS N., CRAIG, ROGER A., and STEPHENSON, JACK D.: Measurements of Thermal Radiation of Air From the Stagnation Region of Blunt Bodies Traveling at Velocities Up to 31,000 Feet Per Second. NASA TM X–508, 1961.
25. WICK, BRADFORD H.: Radiative Heating of Vehicles Entering the Earth's Atmosphere. Paper presented to the Fluid Mechanics Panel of Advisory Group for Aeronautical Research and Development, Brussels, Belgium, April 3–6, 1962.
26. SERBIN, HYMAN: Supersonic Flow Around Blunt Bodies. Jour. Aero. Sci. Readers' Forum, vol. 25, no. 1, Jan. 1958, pp. 58–59.
27. STEPHENSON, JACK D.: A Technique for Determining Relaxation Times by Free-Flight Tests of Low-Fineness-Ratio Cones; With Experimental Results for Air at Equilibrium Temperatures Up to 3440° K. NASA TN D–327, 1960.
28. SEIFF, ALVIN: Secondary Flow Fields Embedded in Hypersonic Shock Layers. NASA TN D–1304, 1962.
29. OSWATITSCH, KLAUS: Similarity Laws for Hypersonic Flow. Tech. Note no. 16, Institutionen för Flygteknik, Kungl. Tekniska Högskolan, Stockholm, 1950.
30. SMITH, WILLARD, G., and PETERSON, WILLIAM P.: Free-Flight Measurement of Drag and Stability of a Blunt-Nosed Cylinder With a Flared After-body in Air and Carbon Dioxide. NASA TM X–642, 1961.
31. PROKOFIEV, V. A.: Consideration of the Effect of Emission of Radiation in the One-Dimensional, Stationary Flow of a Monatomic Gas. Uchenye Zapiski Moskovskogo Gosuderstvennogo Universieteta, Mekhanika, 172, 79, 1952.
32. CLARKE, JOHN F.: Radiation-Resisted Shock Waves. Sudaer no. 121, Stanford University Dept. of Aeronautics and Astronautics, Feb. 1962.

56. Recent Developments in the Chemistry and Thermodynamics of Gases at Hypervelocities

By Thomas N. Canning

THOMAS N. CANNING *is Chief of the Hypervelocity Ballistic Range Branch, NASA Ames Research Center. He earned a B.A. degree from Stanford University in 1943 and an M.S. degree from Stanford in 1947 (mechanical engineering). Mr. Canning developed a mechanical analog for studying the dynamic stability of aircraft; he contributed to understanding of supersonic flows about bodies with fins; he devised novel techniques for hypersonic research on blunt bodies including boundary-layer transition, dynamic stability, and gas-cap radiation; he directed research on hypervelocity impact as applied to meteoroid hazard of spacecraft. Mr. Canning is affiliated with Sigma Xi.*

INTRODUCTION

The day has long since passed when the aerodynamicist working on problems of hypersonic flight could ignore the effects of fundamental physical changes that occur in air at high temperatures. The successive complications that arise beyond those presented by ideal gases, which have translational and rotational degrees of freedom, result from vibration, electronic excitation, dissociation, formation of new molecules, and ionization. The varying rates at which these phenomena occur produce additional complications. The fundamentals of at least a part of these processes are well in hand; for example, the thermodynamic properties of air and other gas mixtures at elevated temperatures may be calculated with great precision.

THERMODYNAMIC AND CHEMICAL PROPERTIES

The details of the calculations and the fundamental spectroscopic work on which the entire theoretical model is based are beyond the scope of the present paper, but an outline of the steps involved may be useful. Emission and absorption spectra of constituents, such as those presented in reference 1, are used to calculate the molecular constants and, subsequently, the partition functions of the atoms and molecules of the particular system in question. The equilibrium constants used for calculating the chemical balance of all anticipated reactions are derived, in turn, from the partition functions. These calculations and the final calculations of chemical reactions are quite laborious, but can be performed, even for complex mixtures, on modern digital computing machines (e.g., ref. 2).

One illustration of results of such computations (as yet unpublished) is shown in figure 56–1. Here the mole fractions of the less common species present in hot mixtures of CO_2 and N_2 are shown as functions of the proportions of CO_2 and N_2 before heating. The reason for selecting this pair of gases was that the atmospheres of Venus and Mars may be composed principally of these two gases. Of particular interest is the production of considerable cyanogen and free carbon, which might result in a significant increment of radiative heating of bodies entering such atmospheres.

666582 O—62——19

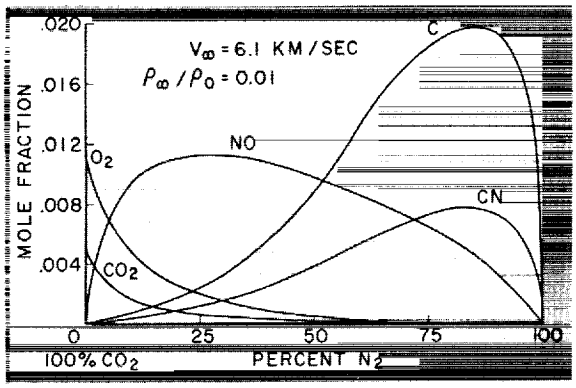

FIGURE 56–1.—Minor-constituent mole fractions behind a normal shock wave in mixtures of nitrogen and carbon dioxide.

TRANSPORT PROPERTIES

The results of the calculations of thermodynamic and chemical properties are straightforward and quite precise, and probably will not require important revision. On the other hand, the transport properties, thermal conductivity, viscosity, Prandtl number, and Lewis number, are not as secure because the details of collisions of the gas particles are not well known.

Efforts have been made, nonetheless, to estimate for engineering purposes the transport properties of air (e.g., Hansen, ref. 3). Some experimental shock tube measurements of thermal conductivity of air have been obtained by Peng and Ahtye (ref. 4). Maecker (ref. 5) has reported conductivity measurements in arc-heated nitrogen.

Peng and Ahtye used the hot stagnant column of gas at the end of a shock tube as shown in figure 56–2. The flow in the shock tube is produced by rupturing a diaphragm, not shown, which separates the driver gas, usually helium, from the driven gas, air. A strong shock wave traverses the length of the air chamber and accelerates the air to high speed. Since the shock tube is closed, the air is stopped by the tube end, and a shock wave passes back through the air producing a hot stagnant region. The equilibrium temperature and density of this air may be accurately calculated from the shock velocity and pressure records. After reflection of the shock wave from the end plate, which contains a thin-film resistance thermometer, there is a transient heat flux from the hot air into the plug. Although the heat-flow rate diminishes rapidly with time, the temperature of the gage surface remains constant at that intermediate temperature to which it jumped, as shown in the inset sketch, until turbulence from the driver gas introduces forced convection. At this time the heat-transfer rate increases and the gage temperature rises. The amount of the temperature jump at the gage surface is a direct measure of the air conductivity integrated over the temperature range between that at the gage surface and the highest air temperature. This feature of the experiment makes the results insensitive to small changes in conductivity at high temperatures because the high resistance to heat flow in the cool air next to the gage tends to dominate the process. Therefore only the integrated theoretical conductivity may be compared to the experimental results.

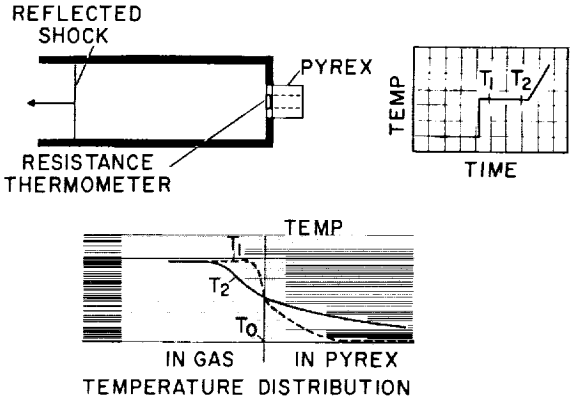

FIGURE 56–2.—Schematic diagram of measurement of integrated thermal conductivity of air in a shock tube.

The integrated thermal conductivity determined experimentally by Peng and Ahtye (ref. 4) is presented in figure 56–3, in the nomenclature of that paper, for comparison with the predictions of Hansen. The agreement observed is quite satisfactory. Any other measurement of heat transfer from gases or liquids to walls also may be used to evaluate the effective conductivity, provided the correct model for heat transfer is used in analyzing the data. Thus the multitude of published shock-tube measurements of heat transfer to models exposed to moving gas, as opposed to the stag-

nant gas samples used by Peng and Ahtye, also may be used to evaluate effective conductivity. The attractive feature of the stagnant-air tests is the simplicity and exactness of the heat-transfer model.

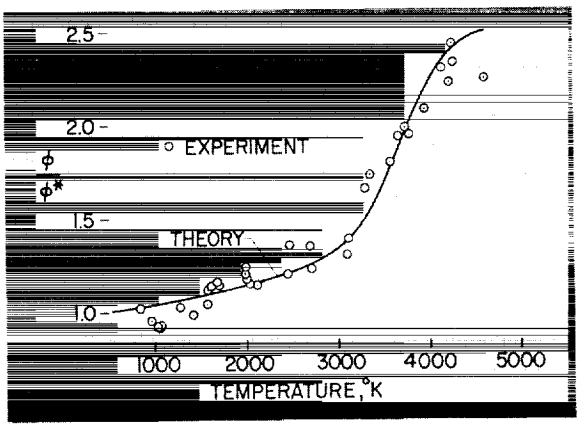

FIGURE 56–3.—Comparison of experimental and theoretical integrated thermal conductivity of shock-heated air.

A radically different experimental approach to this problem which yielded local values of conductivity at high temperature was made by Maecker (ref. 5). He measured the temperature distributions in and near an arc in nitrogen and related the derived gradient at a particular radius to the energy flux from the volume within that radius. The experimental arrangement is shown in figure 56–4. A steady direct-current arc is struck between cathode and anode along a slender channel through a series of cooled copper discs. When steady conditions were obtained, the energy flux per unit of arc length was determined by measuring the arc current and the voltage drop between adjacent insulated copper discs. Since the gas bulk velocity in the apparatus was low, the mechanism of heat flux to the walls was assumed to be laminar conduction (including diffusion of reactive gases) and not forced convection. Radiative effects were also small.

Temperature distributions deduced from emission spectra are presented in figure 56–5.

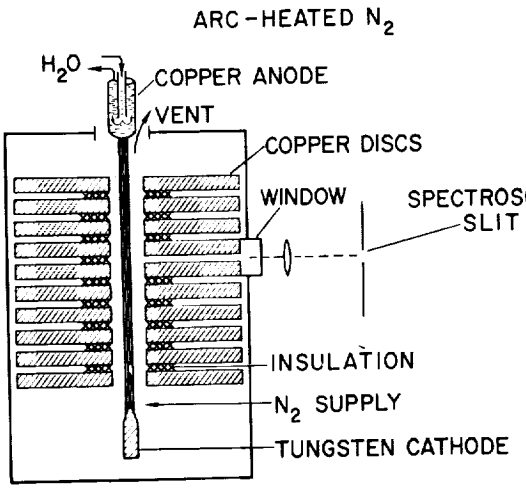

FIGURE 56–4.—Schematic diagram of measurement of local conductivity of nitrogen in an arc.

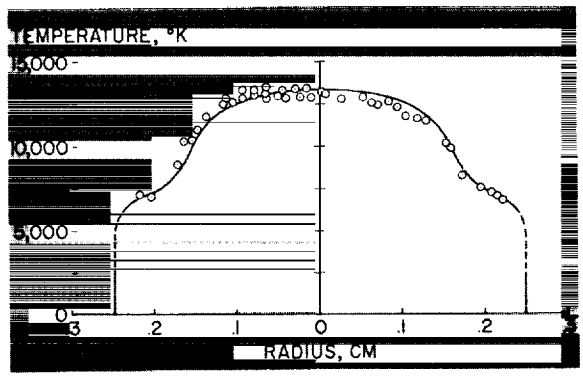

FIGURE 56–5.—Spectrographically measured temperature distribution in and near a direct-current arc in nitrogen.

The low temperature derivatives near the center attest to the exceedingly high thermal conductivity; similarly, the flat portion at 6000° K shows a peak in conductivity. The quantitative results of these tests in N_2 are shown in figure

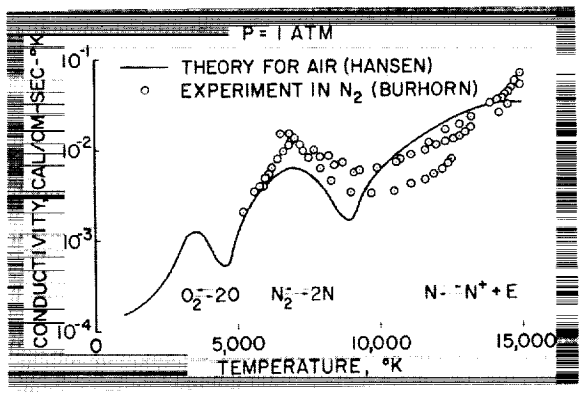

FIGURE 56–6.—Variation of thermal conductivity of nitrogen and air with temperature.

56–6 for comparison with Hansen's prediction for air. The peaks of conductivity correspond to temperature ranges where the rate of formation of the new products noted in the figure with increasing temperature is a maximum. If Hansen's calculations are repeated for pure nitrogen, the peak at 3000° K disappears.

The reason for interest in the thermal conductivity of air and other gases arises naturally from the problem of estimating the aerodynamic heat loads on hypervelocity bodies. Some of the consequences of differing conductivity at high temperatures are discussed by Goodwin (ref. 6).

RADIATIVE PROPERTIES

Another consequence of the excitation of internal degrees of freedom is that if the excited particles return to lower energy states, spontaneously, rather than by virtue of collisions with other particles, they emit radiant energy. At high speeds, this radiation becomes an important part of the heat transferred to body surfaces. In addition to the radiation from hot air within the shock layer, we observe copious radiation from material ablated from heat shields as well. Most of the work done to date by NASA, however, concerns the radiation from air.

The theory of emission of radiant energy from thermally excited atoms and molecules has long been under intensive study and is the subject of many papers. Several such papers (refs. 7, 8, and 9), which are in only reasonable agreement, give values of emissivity of air in chemical and thermodynamic equilibrium at high temperatures for a wide range of densities. These papers are based, in turn, on earlier studies of the chemical constituents of air under the required conditions and on investigations of the particular processes controlling the amount and spectrum of the radiation due to each constituent. The details of these estimates are beyond the scope of the present paper, but predictions from reference 8 of the total radiation per unit volume are shown in figure 56–7 for a broad range of density and velocity. Results derived from references 7 and 9 agree, for the most part within a factor of 2, with those shown in figure 56–7.

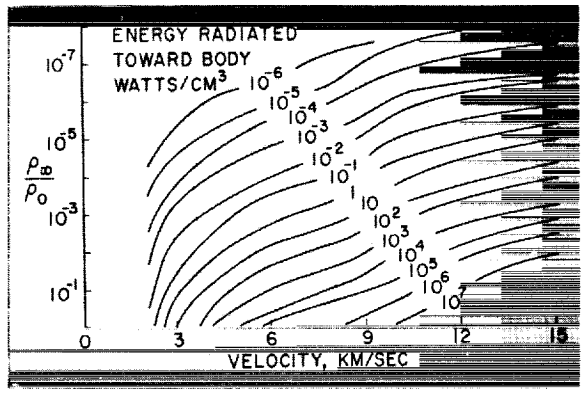

FIGURE 56–7.—Stagnation point equilibrium radiation.

Most of the experimental and theoretical air-radiation work done by industrial and university researchers (e.g., refs. 7–10) has been based on shock tube work while most of that done by NASA at Ames has been done in ballistic-range facilities, reference 11.

The facilities used for the ballistic investigations include small-caliber light-gas guns having muzzle velocities up to 10 kilometers per second. The models are fired into still air or into countercurrent air streams generated by shock-tube-driven wind tunnels having stream velocities up to 5 km/sec. A combined velocity of 13.4 km/sec has been obtained in one facility.

Observations of the radiation from the shock layers of the models are made with photomultiplier tubes; for measurements of the total emitted radiation, broad-band phototubes were used. In most tests several calibrated phototubes were fitted with various narrow-bandwidth optical filters for determining the spectral distribution of the radiation. Figure 56–8 shows schematically the manner in which the models were viewed by the photomultiplier tubes. The inset in this figure is a self-illuminated photograph of the model taken with a Kerr-cell camera with an exposure time of 50 nanoseconds (0.05 microsecond). The velocity of the model relative to the camera for this particular example was 7.9 km/sec. Also shown in the figure is a typical oscilloscope trace of the output of a phototube. The trace records radiation from the hot-gas cap of the model and then of the wake.

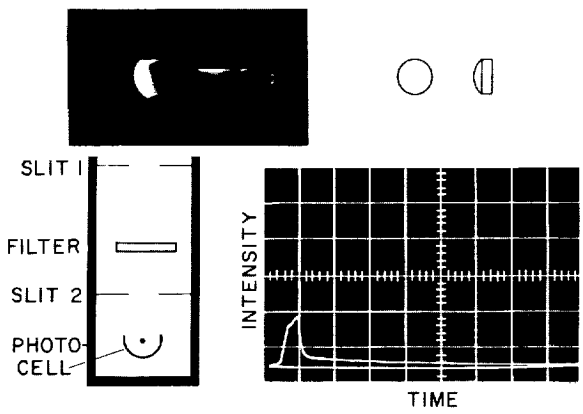

FIGURE 56–8.—Schematic diagram of measurement of radiation from shock layer and wake of hypervelocity projectiles.

Some of the experimental results from the ballistic-range tests are shown in figure 56–9(a), (b), and (c) where the experimentally deduced

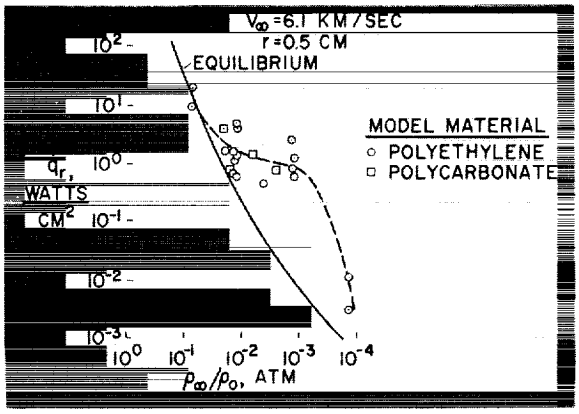

(a) Polyethylene and polycarbonate.

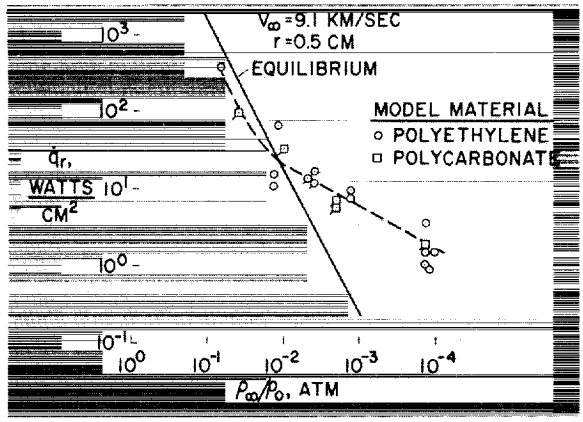

(b) Polyethylene and polycarbonate.

FIGURE 56–9.—Total stagnation-point radiative heating on plastic models.

of important thickness lies between the shock-wave front and the region where the gas is in equilibrium. In one-dimensional flow behind a strong shock wave, it may be argued, following reference 12, that the temperature varies in

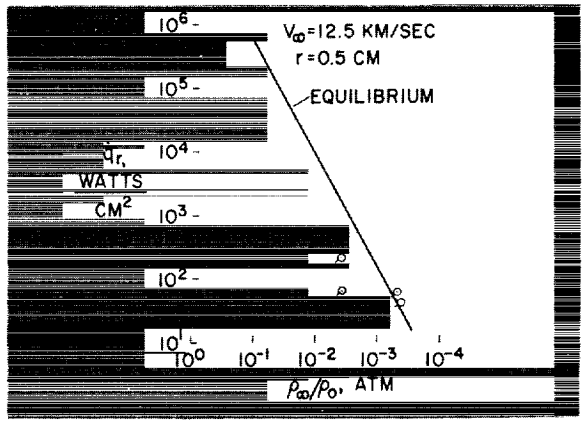

(c) Polyethylene only.

radiative flux on the stagnation regions of the test bodies is compared with predictions based on shock-tube work shown as solid lines. Clearly, the observed radiation exceeds the theoretical levels at ambient densities less than 10^{-2} atmospheres for this model scale at the two lower velocities. The excess radiation is believed to result from nonequilibrium effects which arise because of the finite reaction rates in the disturbed flow field. If the air density becomes low enough, the chemical reaction rates are slowed to such an extent that a reaction zone

a manner such as that sketched in figure 56–10(a). In an exceedingly short distance behind the wave front, the translational temperature reaches a higher than equilibrium value, close to that which would be achieved by a perfect gas. Subsequently, the air relaxes toward thermodynamic and chemical equilibrium, and the temperature reduces to the equilibrium value. In this transient period, collisions produce excited particles that decay to lower states and emit radiation, apparently at rates related to the higher than equilibrium temperatures ex-

isting in this nonequilibrium gas layer. The radiative intensity therefore reaches a value greater than the equilibrium intensity and then reduces to the lower equilibrium value as the gas flows back from the shock front and relaxes to the equilibrium state. In contrast to the high density case depicted in figure 56–10(a), the situation for a lower gas density is depicted in

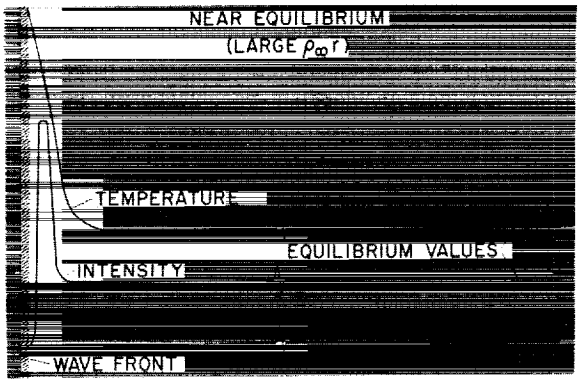

(a) Near equilibrium (large $\rho_\infty r$).

FIGURE 56–10.—Schematic diagram of temperature and radiation as functions of distance behind a strong shock wave.

figure 56–10(b). The relaxation process requires a longer flow distance to achieve completion because the collision rate is reduced if the density is reduced. It can then be seen that greater and greater fractions of the shock layer in front of a body are out of equilibrium and radiate at greater-than-equilibrium radiation levels as the density of the gas in the shock layer is reduced.

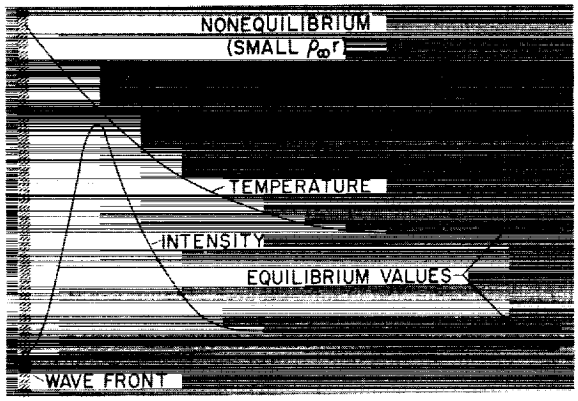

(b) Nonequilibrium (small $\rho_\infty r$).

According to the theory of reaction kinetics, the reaction rates for binary collision processes (which are thought to be controlling in the present case) vary directly with the gas density. On the other hand, the time available for the reactions to occur varies directly with the linear dimension of the flow field. Therefore, if one holds the product of these two quantities constant, that is $\rho_\infty r$ = constant where ρ_∞ is free-stream density and r is a characteristic length of the body, such as the nose radius), the degree of completion of the chemical processes should remain similar between tests made at widely differing scales.

The abrupt reduction at still lower densities noted at 6.1 km/sec is believed to result from one, or a combination of, three effects: first, the reaction rates become so slow that the nonequilibrium radiation does not achieve its full strength before the gas expands around the body; second, the rate of depletion of the excited states by spontaneous decay to lower levels becomes important relative to the collision rate which produces the excited particles (i.e., it is self-extinguishing), and third, the viscous boundary layer becomes so thick that convection to the body reduces the shock-layer temperature and hence the radiation.

One further problem in assessing the importance of radiative heating is to predict and measure the spatial distribution over bodies of interest. The prediction of radiation distribution has been attacked by calculating the density and and temperature variations within the disturbed flow fields with well-known mathematical techniques, such as those discussed in reference 13. The results of such calculations plus the existing data on the radiation from air in thermochemical equilibrium, references 7, 8, and 9, provide the groundwork for the desired estimates. Experimental verification of these estimates is presently being sought in ballistic-range tests. The experimental apparatus is ilustrated in figure 56–11. An orifice plate is imaged, by means of a lens and mirror, into the path of a model which is fired along the range center line. As the projectile flies by, its image traverses the plate and is scanned by one orifice in each column. Behind each column of orifices is placed a thin strip of lucite which acts as a

wave guide for the received light. The strip conducts the light to a photomultiplier for measurement and recording by an oscilloscope. The instrument sketched yields three or four traces on each test. (The vertical spacing of orifices is such that the image can pass between two holes in one column and hence yield no data.) This instrument was devised only recently and has yielded few data. One output trace showing a nearly diametric scan across a spherical model face is shown in figure 56–12.

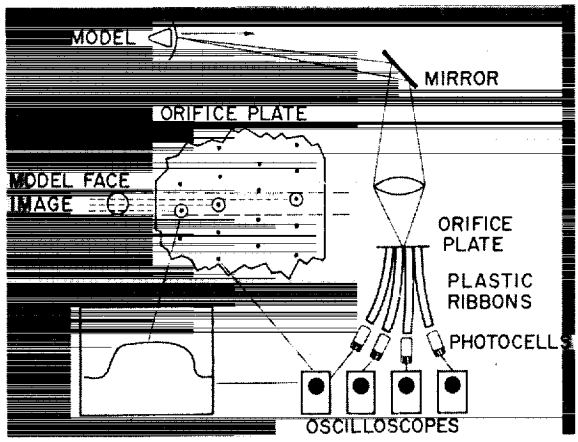

FIGURE 56–11.—Schematic diagram of image dissector for measuring radiation distribution in flow fields of hypervelocity projectiles.

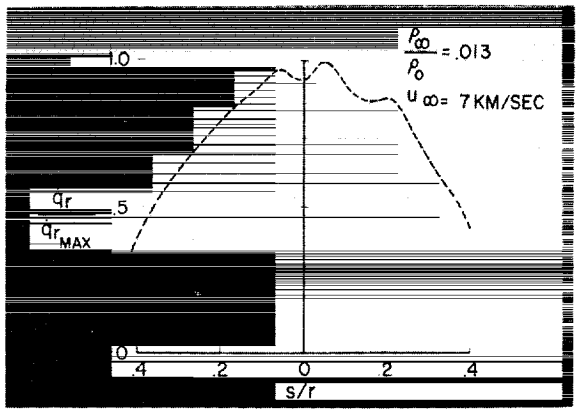

FIGURE 56–12.—Distribution of radiation from the shock layer of a blunt polyethylene projectile.

CONCLUDING REMARKS

All phenomena resulting from high temperatures and their practical ramifications could hardly be treated, even casually, in one paper. The implications of ionization on the thermodynamics and on the attenuation and reflection of microwave energy (the communications blackout and radar cross-section effects) are being studied intensively at many research facilities, academic, industrial, and government. Some of these problems are discussed by Huber (ref. 14). The intense radiation of ultraviolet light by gases behind the bow shock may be absorbed in the flow region ahead of the shock and may produce, in effect, a subsonic-type "warning" to the air that a body is approaching. Study of this complication has begun, as mentioned by Allen (ref. 15), but much work remains to be done.

To bring this discussion full circle, it should be stated that the continued progress in this type of work must be based on more complete understanding of the fundamental properties of the particles, such as collision cross sections, and of the processes which control reaction rates. Only with such theoretical and experimental groundwork will improved understanding and prediction of the observed phenomena be possible.

REFERENCES

1. HERZBERG, G.: Molecular Spectra and Molecular Structure. I. Spectra of Diatomic Molecules. D. Van Nostrand Co., 1950.
2. ZELEZNIK, FRANK J., and GORDON, SANFORD: A General IBM 704 or 7090 Computer Program for Computation of Chemical Equilibrium Compositions, Rocket Performance, and Chapman Jouguet Detonations. NASA TN D–1454, 1962.
3. HANSEN, C. FREDERICK: Approximations for the Thermodynamic and Transport Properties of High-Temperature Air. NASA TR R–50, 1959.
4. PENG, TZY-CHENG, and AHTYE, WARREN F.: Experimental and Theoretical Study of Heat Conduction for Air Up to 5000° K. NASA TN D–687, 1961.

5. MAECKER, H.: Properties of Nitrogen Up to 15,000° K. AGARD Rep. 324, September 1959.
6. GOODWIN, GLEN, and HOWE, JOHN T.: Recent Developments in Mass, Momentum, and Energy Transfer at Hypervelocities. Paper presented at the NASA-University Conference, Chicago, Illinois, Nov. 1–3, 1962.
7. MEYEROTT, R. E., SOKOLOFF, J., and NICHOLLS, R. W.: Absorption Coefficients of Air. LMSD 288052, Lockheed Aircraft Corp., 1959.
8. KIVEL, B., and BAILEY, K.: Tables of Radiation From High Temperature Air. Res. Rep. 21, AVCO-Everett Res. Lab., 1957.
9. BREENE, R. G., NARDONE, MARIA, RIETHOF, T. R., and ZELDIN, SAYDEAN: Radiance of Species in High Temperature Air. Gen. Electric Space Sciences Lab., July 1962.
10. TREANOR, CHARLES E., and MARRONE, PAUL V.: The Effect of Dissociation on the Rate of Vibrational Relaxation. Cornell Aeronautical Lab., Inc., Rep. QM–1626–A–4, Feb. 1962.
11. CANNING, THOMAS N., and PAGE, WILLIAM A.: Measurements of Radiation From the Flow Fields of Bodies Flying at Speeds Up to 13.4 Kilometers Per Second. NASA Paper presented to Fluid Mechanics Panel of Advisory Group for Aeronautical Research and Development, Brussels, Belgium April 3–6, 1962.
12. CAMM, J. C., KIVEL, B., TAYLOR, R. L., and TEARE, J. D.: Absolute Intensity of Nonequilibrium Radiation in Air and Stagnation Heating at High Altitudes. Res. Rep. 93, AVCO-Everett Res. Lab., 1959.
13. SEIFF, ALVIN: Recent Information on Hypersonic Flow Fields. Paper presented at the NASA-University Conference, Chicago, Illinois, Nov. 1–3, 1962.
14. HUBER, PAUL W.: Plasma Frequency and Radio Attenuation. Paper presented at the NASA-University Conference, Chicago, Illinois, Nov. 1–3, 1962.
15. ALLEN, H. JULIAN: Gas-Dynamic Problems of Space Vehicles. Paper presented at the NASA-University Conference, Chicago, Illinois, Nov. 1–3, 1962.

57. Recent Developments in Mass, Momentum, and Energy Transfer at Hypervelocities

By Glen Goodwin and John T. Howe

GLEN GOODWIN *is Chief of the Heat Transfer Branch, NASA Ames Research Center. He earned a B.S. degree from the University of Washington in 1942 (mechanical engineering). He was a U.S. delegate in 1960 to the International Institute of the Aerospace Sciences Conference. Mr. Goodwin is a pioneer in gas dynamics of high-speed rarefied flows; he developed fundamental concepts of hypersonic aerodynamic heating used in design of vehicles such as the X–15; he has directed analytical studies of the chemical state of the flow about reentry vehicles and its dependence on flight trajectory; and he has developed laboratory equipment for producing high-enthalpy rarefied flows. Mr. Goodwin is a member of Sigma Xi.*

INTRODUCTION

The transfer of energy, mass, and momentum by the convective process to surfaces of high-speed vehicles has been studied intensively for many years. A large body of information has been accumulated on the behavior of boundary-layer flows in the speed range where air can be treated as an ideal diatomic gas. The high reentry speeds of space vesicles have introduced complications into these transfer processes which were not considered by the classical boundary-layer theory. These complications are: the interaction with the boundary-layer flows of dissociation and recombination, of ionization and radiation, and of foreign gases from ablation materials. It is the main purpose of this paper to review the effects of these complications on the convective energy transport process and to point out some of the many problem areas which still remain to be solved.

This paper emphasizes the studies of heating rates needed by the space program; skin friction has not been treated directly because the motion of the space vehicles is largely controlled by the pressure drag and not by skin friction. Also, any analysis which treats heat transfer must first solve the momentum equation, and therefore, yields the surface shear forces.

HEAT TRANSFER IN DISASSOCIATED AIR

The first complications to appear as vehicle speeds increase are dissociation and recombination. These phenomena have been treated extensively in the literature and, in particular, in the early papers of Lees and of Fay and Riddell (refs. 1 and 2). The stagnation region of a bluff body is important since it generally has the highest heating rate and is the simplest region to analyze. It is, threfore, interesting to compare the predicted and measured heating rates on the stagnation region of bluff bodies for the speed range where dissociation and recombination are the dominant new phenomena. This comparison is presented in figure 57–1. On the figure are plotted the heating rate normalized with respect to the body nose radius and the stagnation region pressure as a function of the difference between the total enthalpy and

37

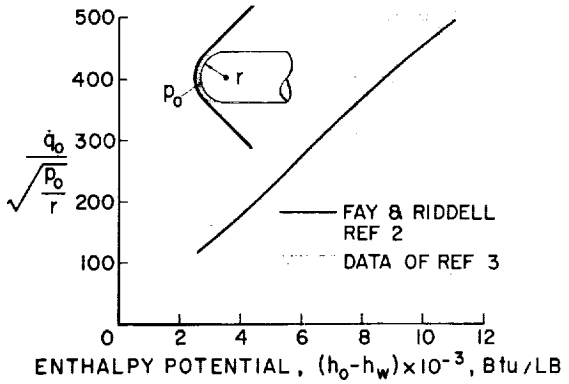

FIGURE 57–1.—Stagnation region heating—equilibrium dissociation.

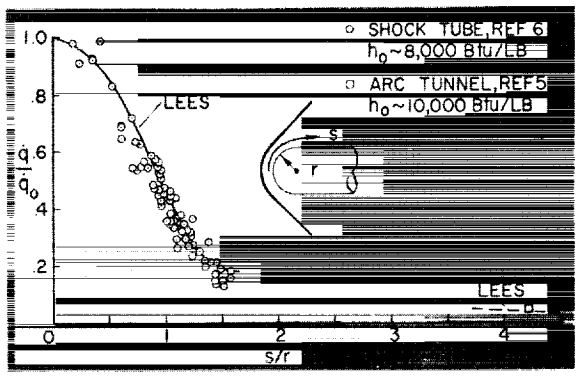

FIGURE 57–2.—Heating rate distribution.

the enthalpy of the wall. The solid-line curve on the figure is the heating rate predicted by Fay and Riddell (ref. 2). The shaded area represents shock tube data of reference 3. Notice that, although there is scatter in the data, the agreement between the theory and the measurements is reasonably good. A large number of measurements have been made in this enthalpy range (see refs. 4 to 6), and the general conclusion is that the prediction method of Fay and Riddell is adequate in this speed range.

Lees, in reference 1, pointed out that the heat-transfer distribution over the body at high Mach numbers could be expressed as a fraction of the stagnation heating, this fraction being mainly a function of the position along the body. A comparison of measured heating rates with the prediction of Lees for hemisphere-cylinder bodies is shown in figure 57–2. On this figure are plotted the heating rates at various positions along the body divided by the value at the stagnation point. Two sets of data are shown here. Shock tube data from reference 6 are shown as the circular symbols, and these are mostly confined to the forward region of the body. Note that the agreement with Lees' prediction is quite good. To the right of the chart is a data point representing a series of measurements at various enthalpy levels of the heating rate downstream of the shoulder of the hemisphere cylinder. Again, the theory of Lees predicts the data quite well.

In order to use Lees' theory, the details of the inviscid flow over the body must be known, but the flow fields over bodies with relatively complicated shapes cannot be easily analyzed. It is possible, however, to measure these flow details and the resulting heating rate experimentally in a conventional high Mach number wind tunnel. The distribution of the heating rate over the body determined by the wind-tunnel tests using a cold gas can then be extrapolated to high enthalpy flows using Lees' theory. My colleague John Reller has verified this method experimentally in the Ames shock tunnel to enthalpy levels of approximately 6,000 Btu/lb, which corresponds to a flight speed of approximately 12,000 ft/sec.

The two figures previously discussed have illustrated the case where the disassociation and recombination time is very short compared to the time the fluid is in the vicinity of the body; hence, the chemical reaction rates can be considered to be in equilibrium everywhere in the flow field. High heating rates are encountered at high altitudes by manned entry vehicles because the deceleration forces must be kept to tolerable levels. The combination of low density, in which the chemical reaction times are long, and high flight speeds is the condition for which one would expect the dissociation and recombination to be out of equilibrium. If the flow time is very short compared with the chemical reaction time, the chemical reactions can be considered frozen. For this condition, energy is transferred to a surface by normal convection and by atoms which diffuse through the boundary layer and recombine on the surface. The question then arises as to the effec-

tiveness of surfaces in promoting the recombination of atoms. On figure 57–3 are shown the stagnation region heating for the case where the boundary layer flow is chemically frozen. Plotted on this chart is the heating rate divided by its equilibrium value, as a function of the total stream enthalpy. Fay and Riddell have shown that if all of the atoms which diffuse to the wall recombined upon it, there would be little change in the gross heating rate to the surface whether the boundary air be frozen or be in equilibrium. This is indicated by the horizontal line. The solid-line curve labeled no recombination at the wall represents the convective portion of the heating from the frozen boundary layer, and the difference between the two curves represents the energy carried by the atoms. Silicon monoxide has a low catalytic efficiency and allows only a small fraction of the atoms to recombine. The data points shown on the figure were obtained on a silicon monoxide surface in a stream of nitrogen gas at sufficiently low pressures and high enthalpy to insure a frozen flow (see ref. 7).

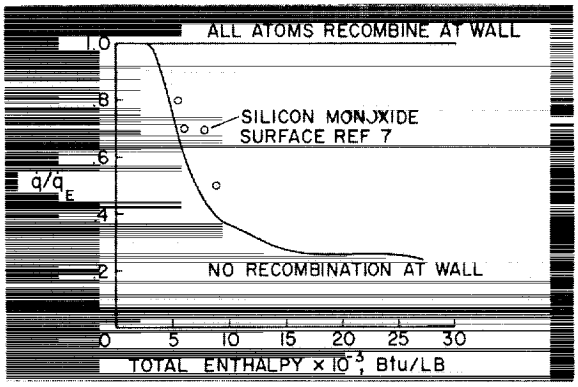

FIGURE 57–3.—Stagnation region—frozen boundary layer.

The reduction in measured heating rate agrees reasonably well with that predicted for the case where no atoms recombined upon the wall. Most metallic surfaces, however, have high catalytic efficiency, and data obtained on copper surfaces lie near the equilibrium value. The question arises as to whether ablating materials will exhibit a high or a low catalytic efficiency for this interesting phenomenon to be exploited. Teflon mass losses measured in a high-enthalpy stream of frozen nitrogen (ref. 5) are about the same as those measured in a stream in equilibrium. This indicates either that teflon has a high catalytic efficiency or that the introduction of teflon vapors into the boundary layer speeds up the recombination reaction. It is interesting to speculate whether or not ablation materials could be found which have a low surface catalysis and, therefore, would receive considerably less incoming heat than surfaces which have been tested.

An important regime to be considered is flight at velocities and altitudes where the boundary layers are neither completely frozen nor in equilibrium. The correlation method presented in reference 8 allows one to determine whether a body is in an equilibrium, a frozen, or a nonequilibrium flight regime when the flight velocity, altitude, and vehicle size are specified. The method essentially is based upon estimating the chemical reaction time compared to the diffusion time of the atoms across the boundary layer. However, this method has not been checked experimentally.

IONIZATION AND RADIATION

As flight speed increases above about 30,000 ft/sec., ionizing reactions take place in the stagnation region flow field. Whether or not the presence of ions and electrons in the flow has a strong influence on convective heat transfer has been the subject of considerable argument. Intuitively, one might feel that the highly mobile electrons would increase the transport of energy by diffusion. Figure 57–4

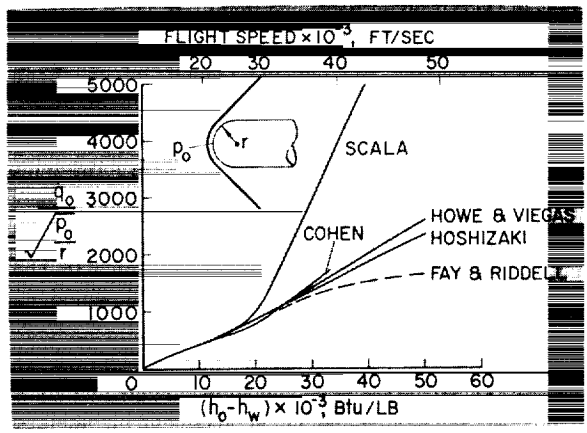

FIGURE 57–4.—Convective heat transfer with ionization.

shows the result of several theoretical efforts to predict the influence of ionization on convective heat transfer in the stagnation region of bluff bodies. Scala (ref. 9) predicts a sharp increase in convective heating at speeds above 30,000 ft/sec. The results of Hoshizaki [1] (ref. 4), Cohen [1] (ref. 10), and Howe and Viegas [1] (ref. 11) indicate that there is no strong ionization effect on convection. The result of Fay and Riddell (ref. 2) for Lewis number of unity is shown for reference, although ionization was not considered in their analysis. Analyses by Pallone and van Tassel (ref. 12), and by Adams (ref. 13) also predict little effect of ionization on convection. Thus, we have a striking difference between the results of Scala and those of other investigators. It appears that the difference in the theoretical results can be attributed to the different methods of treating the transport of energy of reacting species. In particular, the difference appears to be in the total thermal conductivity used by Scala compared to that used by the other investigators. Most of the other investigators have used the transport properties calculated by Hansen in reference 14. A comparison of various calculated transport properties is presented by Fay in reference 15. Theoretical and experimental work in this area is needed to allow the theoretical differences to be reconciled.

Since the theoretical work has not completely settled the question of the effects of ionization on the heating rate, it is of interest to examine the experimental results obtained in this speed range. The comparison is shown on figure 57–5 which uses the same coordinate system as the theoretical comparison. The shock tube experiments of Warren (ref. 16) are in substantial agreement with the Scala theory, while those of Offenhartz (ref. 17), Rose (ref. 3), Stankevics and Rose (ref. 18), and Hoshizaki [2] are in substantial agreement with the other theories (typified by Howe and Viegas). It is much more difficult to determine the reasons for the differences in experimental results than in the theoretical results. Here corrections must be

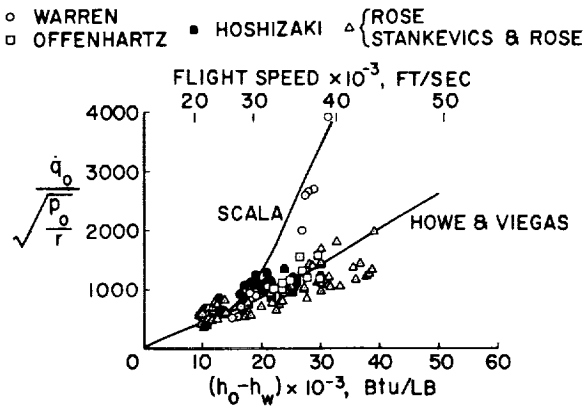

FIGURE 57–5.—Convective heating—comparison with experiment.

made for radiation from the test gas and shock tube driver gas. There is some question concerning the duration of steady-state test time and, of course, questions pertaining to instrumentation. At present, the experimental differences are unresolved, but it is emphasized that these data are very new and the problem is being actively worked on.

In all of the previous discussion, no mention has been made of another phenomenon that influences heat transfer to a large extent at severe flight conditions—a coupling which exists between convection, which is principally a boundary layer effect and gaseous radiation from the flow outside the boundary layer. An analysis by Howe and Viegas (ref. 11) of the entire stagnation region flow field from the body surface to the bow shock wave includes the effects of transport of energy by conduction, diffusion, and radiation in the flow equations. Their results as they affect convective heat transfer (for a stagnation pressure of 1 atm) are shown in figure 57–6. The dashed line represents the convective heat transfer when radiation is neglected in the flow equations. This line is relatively insensitive to changes in nose radius or pressure level and represents a general result when radiative coupling is neglected. The fan of solid lines represents the convective heat transfer when radiation losses from the shock layer are included in the flow equations. It is seen that the effect of radiative coupling reduces the convective heat transfer by about ½ for a body having a 5-foot nose radius.

[1] Compared for a stagnation pressure of one atmosphere; however, little effect of pressure level is evident.

[2] In a private communication, Hoshizaki gives results slightly modified from those of reference 4.

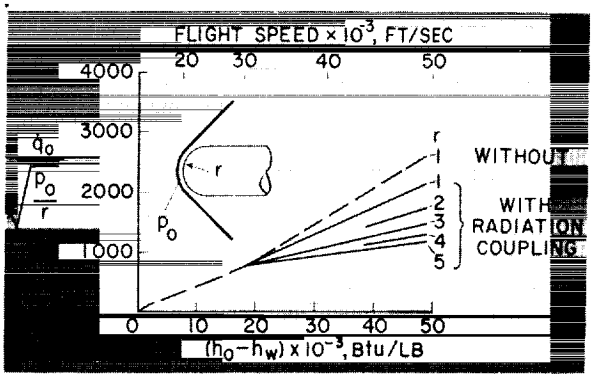

FIGURE 57-6.—Convective-radiative interaction—stagnation region.

Attempts to predict the coupling effect by simple methods have not met with success. The boundary-layer concept apparently breaks down when radiative coupling effects are considered, and the entire flow field must be analyzed. Indeed, flow fields are not clearly divided into a viscous region and an isoenergetic inviscid region characteristic of the lower speeds. This breakdown of the boundary-layer concept has also been shown to occur when the flow is not in chemical equilibrium. (See, e.g., ref. 19.) Generally, it seems that when high speeds occur at high altitudes or when radiation is the predominant form of energy transfer, boundary-layer concepts should be applied with caution.

HEATING RATE IN REGIONS OF SEPARATED FLOW

The preceding section of the paper has been concerned with attached flows; however, the understanding of separated flows has become important because heat transfer to a vehicle surface under a separated flow is frequently less than that to a corresponding attached flow. The Mercury and Apollo spacecraft, for example, take advantage of this fact, and a relatively large portion of the surface of these vehicles is in the separated flow field. An early analysis by Chapman (ref. 20) of the average heating in a cavity covered by a steady separated laminar boundary layer indicated that the average heating rate to the bottom of the cavity should be approximately ½ of its attached flow value. The prediction of this analysis was later confirmed experimentally at moderate Mach numbers. (See refs. 21 and 22.) Later measurements of heating rates to the base of three-dimensional bodies, shaped somewhat like the Mercury spacecraft, have been made at high Mach numbers. The results of a typical test are shown in figure 57-7 wherein the heating rate referred to the forward stagnation-point value is shown as a function of the position along the afterbody. The test was conducted in helium at a Mach number of 15. The solid line curve is the prediction of Chapman, mentioned earlier. It can be seen that this prediction agrees reasonably well with the data and indicates that the early work of Chapman can be used at high Mach numbers. In the test, the flow did not reattach on the afterbody.

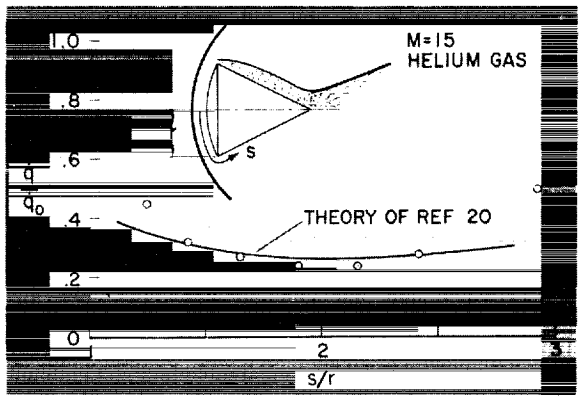

FIGURE 57-7.—Heating in separated region—laminar flow.

When the model in this particular test was positioned at an angle of attack sufficient to cause flow reattachment, the heating rate rose. In fact, the heating rate in the reattached region was higher than that corresponding to a completely attached flow. This is an expected result and has been treated analytically in reference 23 for the case where the flow reattachment angle was perpendicular to the solid surface. In essence, when the separated flow reattaches, it produces a region of high local pressure gradient on the surface, and the high boundary-layer growth rate in this area produces high local heating rates. In the same free stream these reattachment heating rates can be higher than those on a stagnation region of a bluff body with a nose radius roughly equal to the separation length.

The distribution of heating rate along a separated region is generally not analytically predictable at the present time because of our inability to specify the flow details (eddy currents, vortex systems, and flow steadiness) in the separated region. The method of reference 23 will allow heating-rate distributions to be calculated in the separated region if the main features of the flow within the region can be specified. Another problem in this general area that has received little or no attention, at least to the author's knowledge, is that of the effectiveness of transpiration or ablation cooling in a region of separated flow. These are important problems, and certainly worthy of study.

THE EFFECTS OF FOREIGN GASES ORIGINATING FROM SOLID SURFACES ON BOUNDARY-LAYER FLOWS

The preceding portion of this paper has treated clean air flows over reentry bodies but, in practice, the air is almost never uncontaminated. Ablation cooling systems emit a wide variety of foreign gases, and these end up in the boundary layer and in the wake of the body. Generally, little is known about the type or quantity of gas that will be given off by an ablation cooling system because of the types of materials which appear attractive as ablators. These materials are generally mixtures of plastics concocted to achieve a real or fancied result. At the present time, the problem is generally handled by measuring some gross system response, either the amount of material burned away after a timed exposure to a known heating rate or the temperature rise of a portion of a substructure protected by the particular ablation material under study. Some rational results can be obtained, however, on the effect of foreign gases on boundary-layer flows by measuring the change in the heating rate or skin friction resulting from transpiring measured amounts of gases of known properties and composition through porous model surfaces. The results of one such study made by C. Pappas of Ames are shown in figure 57–8. On this figure is plotted the heating rate divided by its value for no transpiration as a function of the transpiration flow rate per unit area times the

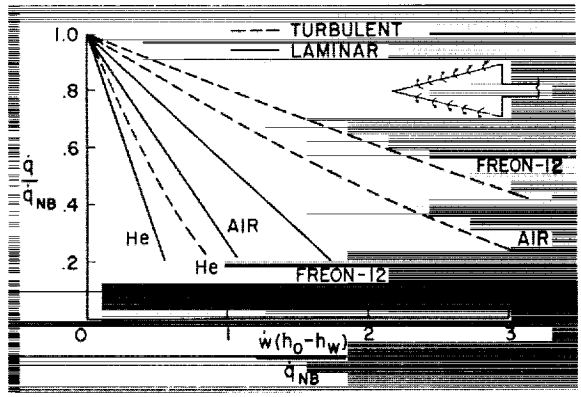

FIGURE 57–8.—Effect of foreign gas transpiration on heating rate.

driving enthalpy potential divided by the heating rate for zero transpiration. This particular coordinate system is used because it accounts for the major effects of Mach number and Reynolds number on test results of this type. For a particular flight condition, the abscissa is proportional to the weight flow of the foreign gas transpired through the porous surface. Two sets of results are shown. The solid lines are for the behavior of a laminar boundary layer, and the dashed lines are for the behavior of a turbulent boundary layer. The results of the laminar-flow tests will be examined first. Three gases were transpired: helium, a light gas having a molecular weight of 4; air, having a molecular weight of 29; and freon, a heavy gas having a molecular weight of 121. Notice generally that the light gases are more effective than the heavy gases in reducing the heating rate, and a large reduction in heating rate results from rather small transpiration rates. Typically the ratio of the mass-flow rate of the transpired gas to the mass-flow rate of the free stream per unit area is about 0.001.

The turbulent boundary layer results are not so dramatic as the laminar flow results, but the trends are similar.

At very high blowing rates from ablating surfaces the heating rates do not go to zero as indicated by a simple extrapolation of the results shown on figure 57–8. For laminar flow, high blowing rates cause transition and, for turbulent flow, high blowing rates appear to destroy boundary-layer character of the flow. It is, therefore, difficult to make any general

statements about the asymptotic values of the heating rate for very large blowing rates. Some work has been done along this line, however, and is reported in reference 24. These test results were obtained indirectly from the ablation of teflon and they show an asymptotic heating rate for laminar flow of approximately 0.18 of its no-blowing value. Work is needed to extend transpiration test results to other gases and to higher enthalpy flows.

TURBULENT BOUNDARY LAYER AT HIGH ENTHALPIES

Theoretical predictions of the behavior of a turbulent boundary layer have depended largely upon experiment to evaluate critical assumptions, fundamentally, because the turbulent boundary layer is a more complicated phenomenon than the laminar boundary layer, and no complete solutions to the turbulent boundary-layer equations have been obtained. Progress that has been made generally resulted from transformations such as those given in reference 25 which allow one to transform turbulent compressible boundary-layer equations into their equivalent incompressible form. These transformations are valuable in that they allow the well-known low velocity profiles and the matching point between the laminar sublayer and the outer turbulent layer to be extrapolated to the compressible flow case. However, these methods give no hint of the effect of increasing stream enthalpy level on the skin friction or the heat transfer.

Historically, the effects of temperature or enthalpy level on the heating rate and skin friction produced by turbulent boundary layers have been handled by a method analogous to that used to correlate skin friction and heating rate from turbulent flows in pipes. This method uses a reference temperature intermediate between the wall surface and the bulk of the fluid at which to evaluate the fluid properties to account for temperature level effects. For the case of undissociated air at relatively high Mach numbers, the reference temperature method has been used successfully in aerodynamics to correlate experimental results of skin friction and heating rate. The methods are described and compared with experiments in references 26 and 27. At still higher flight speeds where dissociation becomes important, Eckert, reference 28, has suggested evaluating the fluid properties at a reference enthalpy, which lies intermediate between the enthalpy at the wall and the enthalpy of the gas at the boundary-layer edge. The details of this method are given in reference 29, but it is, in essence, similar to the older reference temperature method. These methods, as crude as they are, do a reasonably good job of correlating experimental data. They are, however, disappointing in the sense that they do not shed any real understanding on the basic changes in the turbulent transport mechanism with increasing enthalpy. A typical set of experimental data is compared with the reference enthalpy method on figure 57-9. On this figure are plotted the heating rate divided by the $(R)^{4/5}$, which is the parameter used for low-speed turbulent boundary layer flows to account for the Reynolds number variation of the data. This parameter is plotted as a function of the total stream enthalpy. The circular points are experimentally measured values of this parameter obtained in a shock tube and reported in reference 30. The reference enthalpy method of Eckert is shown as the solid-line curve. Notice that the data generally fall below the prediction as is characteristic of this method when applied at lower enthalpies; that is, the method generally is conservative and overestimates the heating rate somewhat. However, it has been found extremely useful for engineering applications.

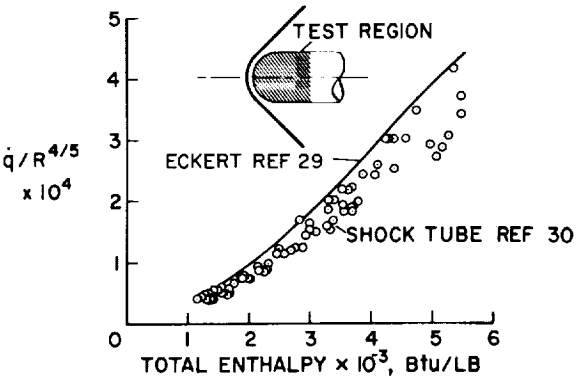

FIGURE 57-9.—Heating in turbulent flow at high enthalpy.

Further progress in the field of predicting heat-transfer rate or skin friction produced by a turbulent boundary layer awaits the development of experimental apparatus capable of producing high enthalpies at sufficiently high pressures to produce a fully developed turbulent flow.

Another problem area essentially unsolved even for low speed is the prediction of the point of transition between a laminar and a turblent flow. Probably no other area of research in aerodynamics has received so much attention from so many people. In spite of the large amount of work expended on this subject, only a few general rules have emerged. These rules were stated by Osborne Reynolds and have remained essentially unchanged up to the present time. The rules are that if the Reynolds number is less than about 1 million, the flow will probably be laminar; if the Reynolds number is greater than approximately 10 million, then the flow will generally be turbulent. If the Reynolds number of the flow lies between these two rather generous boundaries, then the flow will be laminar, transitional, or turbulent, depending upon the particulars, the discussion of which is outside the scope of this paper. Generally, the body surface roughness, the pressure gradient, the wall temperature, and the history of the flow as it proceeds over the body influence the transition. The situation is further complicated when the enthalpy of the flow is increased. At the present time, transition information must be collected from flight tests which are expensive and which do not lead to generalizations. The ballistic range has proven a very useful tool to study transition at lower speeds, and the development of techniques to detect transition in the newer ballistic range shock tunnels would allow this problem to be studied at the higher speeds of present interest.

Yet another complication is introduced when foreign gases are ablated into the boundary layer. Results obtained from porous cones tested in wind tunnels over a relatively wide Mach number range with various foreign gases transpired through the surface give some hint as to the influence of this phenomenon on transition. These tests have indicated that the introduction of a foreign gas into the boundary layer reduces the Reynolds number of transition; however, the Reynolds number of transition does appear to reach an asymptotic value beyond which further surface blowing has little effect. In the particular set of tests reported in reference 31, this asymptotic value of the transition Reynolds number was about 1.75 million, as compared to a transition Reynolds number of 3.3 million on the same body without transpiration.

HEATING RATES IN PLANETARY ATMOSPHERES

Currently planned entry into the atmosphere of the nearby planets emphasizes the need for research in gases other than air. The atmospheres of the two planets nearest the earth, Mars and Venus, consist of mixtures of nitrogen and carbon dioxide, but the particular composition of these atmospheres is not known with great precision at present; however, it is interesting and informative to compare the heat-transfer results in pure carbon dioxide and see whether they are greatly different from those experienced in air.

It is known (see refs. 32 and 33) that carbon dioxide dissociates at relatively low temperatures and that the recombination of carbon monoxide back to its carbon dioxide state is a very slow process. The temperatures at which carbon monoxide and nitrogen dissociate are not greatly different. It is reasonable to conclude, therefore, that the fluid contained in the boundary layers of vehicles flying in atmospheres rich in carbon dioxide and nitrogen will have as their main constituents nitrogen, carbon monoxide, and atomic oxygen at the lower speeds and the atomic products of the dissociation of these gases at higher speeds. The collision diameters and molecular weights of the CO_2-N_2 mixtures are similar to air at elevated temperatures; therefore, it is reasonable to expect that the transport properties will be similar. Hoshizaki (ref. 4) has made this comparison and finds that the viscosity and total thermal conductivity are not too different. Using these transport properties, he solved the laminar boundary layer equations for the stagnation region of a blunt body in carbon dioxide and found that the heating rates should not differ

from those predicted for air by more than about 10 percent. It is interesting now to compare the measured and predicted heating rates in carbon dioxide with those in air to see whether these predictions are borne out. These comparison is shown on figure 57–10 where the heating rate is plotted as a function of the difference between the total enthalpy and the wall enthalpy. Two theoretical lines are shown. The upper line is the theory of Scala (ref. 34), and the lower line is the theory of Hoshizaki (ref. 4). Shown on the figure also are the various measurements that have been made. The lower set of points was obtained in a free-flight range and is described in detail in reference 35. The middle set of points was obtained by Rutowski and Chan, reference 36. The data represented by the circular points were obtained in the General Electric Hypervelocity Shock Tube. It can be seen that up to about 25,000 ft/sec the experimental data agree quite well with either prediction; at the higher speeds the data lie intermediate between the two theories. Also shown on the chart as a shaded area is the air data taken from figure 57–4, and it can be seen that it agrees with the carbon dioxide data reasonably well. It appears then, that to a first approximation the heating rates in carbon dioxide are about the same as the heating rates for air.

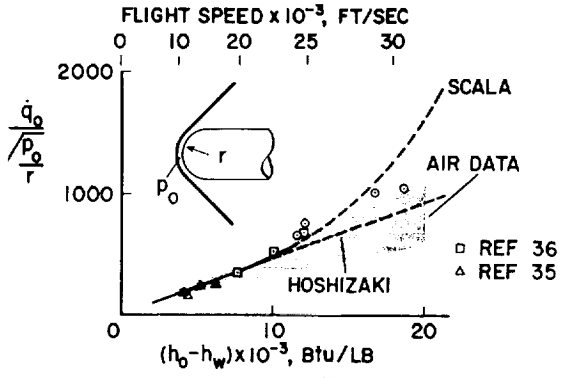

FIGURE 57–10.—Comparison of heating rate in air and carbon dioxide.

There is no information, to the authors' knowledge, of heating-rate distribution over a body in carbon dioxide or in carbon dioxide and nitrogen mixtures. However, based on the similarity of the transport properties and the considerations outlined by Lees in reference 37, one would not expect marked deviation from the results obtained with air. This conjecture, however, should most certainly be checked experimentally.

RÉSUMÉ

The primary points of this survey are:

(1) Methods are generally available which account reasonably well for the behavior of the laminar attached boundary layer up to speeds corresponding to the onset of ionization.

(2) Although the effect of ionization on convective heat transfer has yet to be determined conclusively, most of the theoretical and experimental results indicate that the effect is small.

(3) The structure of the flow field loses the appearance of a boundary layer joined to an isoenergetic inviscid region.

(a) at high altitude because of chemical effects and

(b) at high speed because of radiative transport.

The conclusion is that at these conditions the entire flow field should be analyzed without dividing it into a boundary layer and an isoenergetic inviscid shock layer.

(4) Heating rates to the stagnation region of bluff bodies in carbon dioxide are essentially the same as those in air.

(5) The largest area of uncertainty in flow-field analysis is concerned with the effects of contamination on energy transport phenomena. In particular, the influence of the high enthalpy on the thermochemistry and of ionization on the flow field containing foreign gases needs intensive investigation.

(6) Experimental and theoretical work needs to be done on transition and on the turbulent boundary layer in high enthalpy flows.

SYMBOLS

h	static enthalpy, Btu/lb
M	Mach number
p	pressure, atm
q	heating rate, Btu/ft²sec
r	nose radius, ft

R Reynolds number based on edge properties
s coordinate along body measured from stagnation point, ft
w mass rate of injection, lb/sec ft^2

Subscripts:
E equilibrium
NB no blowing
O stagnation conditions
w conditions at the wall

REFERENCES

1. Lees, L.: Laminar Heat Transfer Over Blunt-Nosed Bodies at Hypersonic Flight Speeds. Jet Propulsion, vol. 26, no. 4, April 1956, pp. 259–269, 274.
2. Fay, J. A., and Riddell, F. R.: Theory of Stagnation Point Heat Transfer in Dissociated Air. Jour. Aero. Sci., vol. 25, no. 2, Feb. 1958, pp. 73–85, 121.
3. Rose, P. H., and Stark, W. I.: Stagnation Point Heat-Transfer Measurements in Dissociated Air. Jour, Aero, Sci., vol. 25, no. 2, Feb. 1958, pp. 86–97.
4. Hoshizaki, H.: Heat Transfer in Planetary Atmospheres at Super-Satellite Speeds. ARS Journal, vol. 32, no. 10, Oct. 1962, pp. 1544–51.
5. Vojvodich, Nick S.: The Performance of Ablative Materials in a High-Energy, Partially Dissociated Frozen Nitrogen Stream. NASA TN D–1205, 1962.
6. Kemp, Nelson H., Rose, Peter H., and Detra, Ralph W.: Laminar Heat Transfer Around Blunt Bodies in Dissociated Air. Jour. Aero/Space Sci., vol. 26, no. 7, July 1959, pp. 421–430.
7. Winkler, Ernest L., and Griffin, Roy N., Jr.: Effects of Surface Recombination on Heat Transfer to Bodies in a High Enthalpy Stream of Partially Dissociated Nitrogen. NASA TN D–1146, 1961.
8. Goodwin, Glen, and Chung, Paul M.: Effects of Nonequilibrium Flows on Aerodynamic Heating During Entry into the Earth's Atmospheres from Parabolic Orbits. Advances in Aero. Sci., vol. 4, Pergamon Press, New York, 1961, pp. 997–1018.
9. Scala, Sinclaire M., and Warren, Walter R.: Hypervelocity Stagnation Point Heat Transfer. Gen. Elec. Space Sci. Lab., R61SD185, 1961.
10. Cohen, Nathaniel B.: Boundary-Layer Similar Solutions and Correlation Equations for Laminar Heat-Transfer Distribution in Equilibrium Air at Velocities up to 41,000 Feet per Second. NASA TR R–118, 1961.
11. Howe, J. T., and Viegas, J. R.: Solutions of the Ionized Radiating Shock Layer Including Reabsorption and Foreign Species Effects and Stagnation Region Heat Transfer. Prospective NASA TR, 1963.
12. Pallone, A., and Van Tassell, W.: Stagnation Point Heat Transfer for Air in the Ionization Regime. ARS Journal, vol. 32, no. 3, March 1962, pp. 436–7.
13. Adams, Mac C.: A Look at the Heat Transfer Problem at Super-Satellite Speeds. ARS Paper No. 1556–60, American Rocket Society, New York, December 1960.
14. Hansen, C. Frederick: Approximations for the Thermodynamic and Transport Properties of High-Temperature Air. NASA TR R–50, 1959.
15. Fay, James A.: Hypersonic Heat Transfer in the Air Laminar Boundary Layer. Presented at Hypersonic Specialists Conference, AGARD, Brussels, Belgium, 1962.
16. Warren, W. R., Rogers, D. A., and Harris, C. J.: The Development of an Electrically Heated, Shock Driven Test Facility. Second Symposium on Hypervelocity Techniques, Denver, 1962.
17. Offenhartz, E., Weisblatt, H., and Flagg, R. F.: Stagnation Point Heat Transfer Measurements at Super Satellite Speeds. Jour. of the Royal Aero. Soc., vol. 66, no. 613, January 1962, p. 54.
18. Stankevics, J. O. A., and Rose, P. H.: Measurements of Stagnation Point Heat Transfer in Partially Ionized Air. Paper to be presented at IAS Meeting, January 1963.
19. Chung, Paul M.: Hypersonic Viscous Shock Layer of Nonequilibrium Dissociating Gas. NASA TR R–109, 1961.
20. Chapman, Dean R.: A Theoretical Analysis of Heat Transfer in Regions of Separated Flow. NACA TN 3792, 1956.
21. Larson, Howard K.: Heat Transfer in Separated Flows. Jour. Aero/Space Sci., vol. 26, no. 11, November 1959, pp. 731–738.
22. Chapman, Dean R., Kuehn, Donald M., and Larson, Howard K.: Investigation of Separated Flows in Supersonic and Subsonic Streams With Emphasis on the Effect of Transition. NACA TN 3869, 1957.

23. CHUNG, PAUL M., and VIEGAS, JOHN R.: Heat Transfer in the Reattachment Zone of Separated Laminar Boundary Layers. NASA TN D–1072, 1961.
24. LUNDELL, JOHN H., WINOVICH, WARREN, and WAKEFIELD, ROY M.: Simulation of Convective and Radiative Entry Heating. Advances in Hypervelocity Technique, Plenum Press, New York, 1962, pp. 729–748.
25. VAGLIO-LAURIN, ROBERTO: Turbulent Heat Transfer on Blunt-Nosed Bodies in Two-Dimensional and General Three-Dimensional Hypersonic Flow. Jour. Aero/Space Sci., vol. 27, no. 1, January 1960, pp. 27–36.
26. SOMMER, SIMON C., and SHORT, BARBARA J.: Free-Flight Measurements of Turbulent-Boundary-Layer Skin Friction in the Presence of Severe Aerodynamic Heating at Mach Numbers from 2.8 to 7.0. NACA TN 3391, 1955.
27. TENDELAND, THORVAL: Effects of Mach Number and Wall-Temperature Ratio on Turbulent Heat Transfer at Mach Numbers from 3 to 5. NASA TR R–16, 1959.
28. ECKERT, ERNEST R. G.: Survey on Heat Transfer at High Speeds. WADC Technical Report 54–70, 1954.
29. ECKERT, ERNST R. G.: Survey of Boundary Layer Heat Transfer at High Velocities and High Temperatures. WADC Technical Report 59–624, 1960.
30. ROSE, PETER H., ADAMS, MAC C., PROBSTEIN, RONALD F.: Turbulent Heat Transfer on Highly Cooled Blunt Nosed Bodies of Revolution in Dissociated Air. Heat Transfer and Fluid Mechanics Institute, 1958, pp. 143–155.
31. PAPPAS, CONSTANTINE C., and OKUNO, ARTHUR F.: Measurements of Skin Friction of the Compressible Turbulent Boundary Layer on a Cone with Foreign Gas Injection. Jour. Aero/Space Sci., vol. 27, no. 5, May 1960, pp. 321–333.
32. RAYMOND, J. L.: Thermodynamic Properties of Carbon Dioxide to 24,000° K with Possible Application to the Atmosphere of Venus, RM–2292, The Rand Corporation, November 1958.
33. STEINBERG, MARTIN, and DAVIES, WILLIAM O.: The Oxidation of Carbon Monoxide Behind Shock Waves. ARL Tech. Rep. 60–312, Armour Research Foundation, December 1960.
34. SCALA, S. M.: Heating Problems of Entry into Planetary Atmospheres from Supercirular Orbiting Velocities. General Electric Space Science Laboratory, R61SD176, 1961.
35. YEE, LAYTON, BAILEY, HARRY E., and WOODWARD, HENRY T.: Ballistic Range Measurements of Stagnation-Point Heat Transfer in Air and in Carbon Dioxide at Velocities up to 18,000 Feet per Second. NASA TN D–777, 1961.
36. RUTOWSKI, R. W., and CHAN, K. K.: Shock Tube Experiments Simulating Entry into Planetary Atmospheres. LMSD–288139, Lockheed Missiles and Space Co., January 1960.
37. LEES, LESTER: Convective Heat Transfer with Mass Addition and Chemical Reactions. Paper presented at Third Combustion and Propulsion Colloquim, AGARD, NATO Palermo, Sicily, 1958. Pergamon Press (California Institute of Technology, Pub. 451).